TO: R. HAWRYLUK, C. NEUMEYER
FROM: S.P. GERHARDT (PPPL), M.L. REINKE (ORNL)
SUBJECT: HEAT FLUXES ON THE INBOARD DIVERTOR VERTICAL REGION

1: Intent

The intent of this memo is to document the heat flux related requirements on the plasma facing components (PFCs) for the Inboard Divertor Vertical (IBDV), complementing other documents that describe the same for the Center Stack Angled Section (CSAS), Inboard Divertor Horizontal (IBDH) and Outboard Divertor (OBD) [1,2] surfaces. Specific requests from Topical Science Groups (TSGs) are included [3-8], as are additional scans motivated by those requests.

2: Conclusions

IBDV	**Case# ->**	**1**	**2**	**3**	**4**
Range of Application	m	1.27< |Z| < 1.5	1.27< |Z| < 1.5	|Z|>1.5	|Z| > 1.27
Max Angle	degrees	5.5	6.0	4.0	-1
Min Angle	degrees	2.0	2.0	1.0	-5
Heat Flux	MW/m^2	5.0	10	3.5	1
Duration	s	5	1	5	1
Reference		High I_p and B_T DN w/ Sweeping (Table 5.6)	LSN Sweeping (Table 5.5)	Spill Over from Scans in HHF region	Reversed Helicity Requirement (Section 6)

***Table 2.1**: Suggested heat flux requirements for IBDV surface*

The various use cases for the IBDV can be reduced to the following requirements shown in Table 2.1. Section 5 outlines the decision making process for Case#1 and Case#2 requirements and describes the discharges in more detail. These both utilize strikepoint sweeping to lower time-averaged heat flux. Section 4 outlines stationary LSN and DN discharges where it was found that at high power and I_p=2 MA, B_T= 1 T, peak IBDV heat fluxes were above 7 MW/m^2, anticipated to be beyond designs using isotropic graphite. Through analysis of TSG requests and further investigation, it was found that the PF1a coil location prevents the strike point from reaching the lower portion, |Z| > 1.5 [m], of the IBDV surface. This results in a lower heat flux requirement for this region, with Case#3 in Table 2.1 representing the effect of power from the high heat flux regions spilling over into the lower heat flux regions, for instance in DivSOL 8-05. This is discussed in more detail in Section 7. The Case#4 requirement is based on needing to handle a marginal amount of power in the reversed helicity to support DivSOL TSG research.

It is worth noting that uncertainty in specifying inner divertor heat fluxes are rather large, even relative to the outer divertor, and models are intended to give conservative predictions. To enhance radiation in the divertor, a requirement for private flux region gas fueling has been added. A detailed post-Recovery commissioning plan is necessary to help validate heat flux models and update NSTX-U operating space accordingly.

3: Methods

The methods in this memo are described in Section 3 of the memo *Heat Fluxes on the CSAS and Far OBD Region* [1]. Note that the Heuristic Drift Scaling of the SOL width is used, and a 30% radiation fraction is assumed. Both of these are likely to be conservative

assumptions, i.e. provide large projected heat fluxes. Calculations are based on the original NSTX-U PFC boundary. If that boundary is moved as in the expected CDR designs, the heat fluxes for the chosen equilibria may change.

4: Stationary H-modes

4.1: Double-Null Cases

Double-null (DN) equilibria are up-down symmetric, with an X-point on the boundary at both the top and bottom of the equilibrium. These will have the lowest heating on the vertical targets. This section describes double-null equilibria that were requested by the ASC[4] and DivSOL[3] TSGs in the TSG survey.

4.1.1: DN Scans from the DivSOL TSG

A series of cases were run at elongation of 2.25 and high triangularity of 0.6; the ISP lands at approximately Z=+/- 1.32 m. In all cases, there is a radiated power fraction of 30%, with 10% of the remaining power going each of the lower or upper inner targets. Figure 4.1.1.1 show example equilibria, where these modest elongations will also deposit some 'spillover' power onto the CSAS as discussed in Section 5 of [1].

Quantity	Units	Value
elongation	---	2.25
lower triangularity	---	0.6
upper triangularity	---	0.6
dr_{sep}	cm	0
$\|Z_{ISP}\|$	m	1.32

***Table 4.1.1.1**: Common parameters for the DivSol DN scans in this section*

The heat fluxes from these I_P and B_T scans are listed in Table 4.1.1.2 (see Section 4.2 for more explanation on the how these data are derived). From Table 4.1.1.2, it appear that even in perfect double null, power fluxes exceeding 10 MW/m^2 are possible within present model assumptions (e.g. 30% radiated power). Despite a small fraction of the input power being delivered to the inner strike point, it is difficult to consistently achieve small angles of incidence due to limited influence by the PF1 coil set.

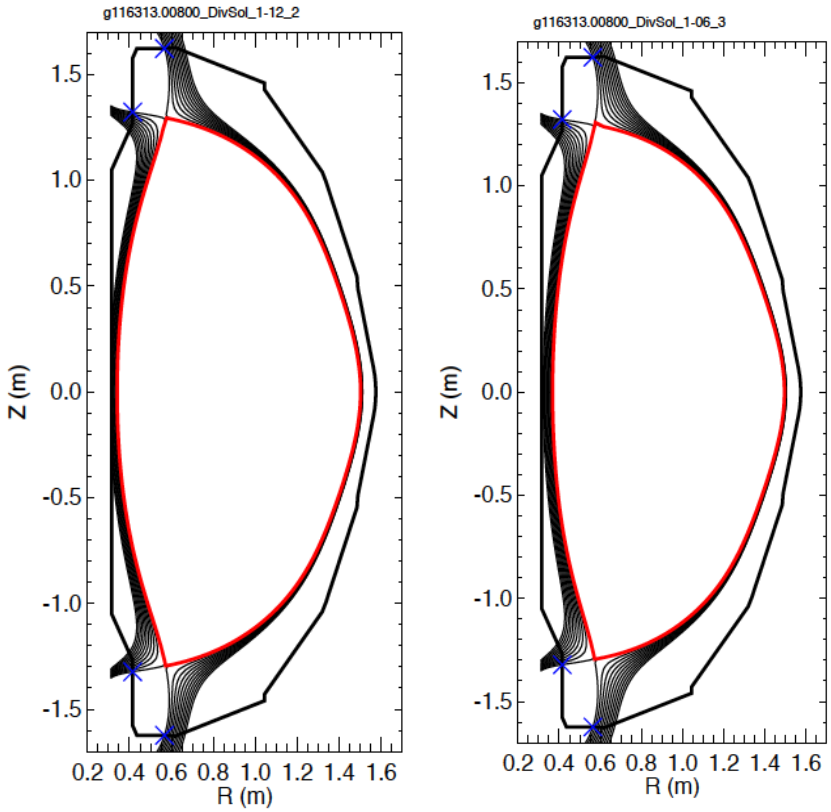

***Fig. 4.1.1.1**: Representative DN equilibria discussed in this section*

DivSol Scans	I_P	B_T	P_{inj}	q_{peak}	Angle at Peak
	MA	T	MW	MW/m^2	degrees
1-01	0.5	0.5	3	0.8	3.0
1-02	1.0	0.5	4	2.8	7.2
1-05	0.5	0.75	3	0.6	1.8
1-06	1.0	0.75	5	3.2	4.5
1-07	1.5	0.75	7	7.5	7.2
1-09	0.5	1.0	4	0.7	1.1
1-10	1.0	1.0	7	3.8	3.2
1-11	1.5	1.0	9	8.5	5.2
1-12	2.0	1.0	10	12.7	7.2

***Table 4.1.1.2**: Common parameters for the DivSol DN scans in this section.*

4.1.2 DN Scans from ASC TSG

The ASC TSG requested a series of DN scans. While the initial request was for cases with elongations of 2.4, these were augmented by cases with elongations of 2.6. These include cases at the highest current, I_p=2.0 MA and field, B_T=1.0 T, expected for NSTX-U, over a range of input powers.

gfile name	I_P	B_T	P, NBI	q_{peak}	Angle
--	MA	T	MW	MW/m^2	degrees
g116313.00860_ASC_S-01	1.0	0.5	7.5	4.6	6.0
g116313.00860_ASC_S-02	1.2	0.5	8.0	6.0	7.1
g116313.00860_ASC_S-03	1.4	0.5	8.5	8.0	8.6
g116313.00860_ASC_S-07	1.0	0.75	7.5	4.2	3.9
g116313.00860_ASC_S-08	1.2	0.75	8.0	5.8	4.8
g116313.00860_ASC_S-09	1.4	0.75	8.5	7.5	5.7
g116313.00860_ASC_S-10	1.6	0.75	9.0	9.1	6.3
g116313.00860_ASC_S-11	1.8	0.75	9.5	11.2	7.2
g116313.00860_ASC_S-12	2.0	0.75	10.0	13.4	8.0
g116313.00860_ASC_S-13	1.0	1.0	7.5	3.7	2.7
g116313.00860_ASC_S-14	1.2	1.0	8.0	4.8	3.1
g116313.00860_ASC_S-15	1.4	1.0	8.5	6.4	3.8
g116313.00860_ASC_S-16	1.6	1.0	9.0	8.2	4.4
g116313.00860_ASC_S-17	1.8	1.0	9.5	10.1	5.1
g116313.00860_ASC_S-18	2.0	1.0	10.0	12.4	5.8

Table 4.1.2.1*: Parameters of the ASC scan at elongation of 2.3 and triangularities of 0.65. The height of the inner strikepoint is Z=-1.33 in these equilibria.*

gfile name	I_P	B_T	P, NBI	q_{peak}	Angle
--	MA	T	MW	MW/m^2	degrees
g116313.00860_ASC_T-01	0.75	0.5	6.0	1.6	2.7
g116313.00860_ASC_T-02	1.0	0.5	7.0	2.5	3.5
g116313.00860_ASC_T-03	1.25	0.5	8.0	4.0	4.6

g116313.00860_ASC_T-04	1.5	0.5	9.0	5.7	5.7
g116313.00860_ASC_T-07	0.75	0.75	6.5	1.4	1.6
g116313.00860_ASC_T-09	1.25	0.75	8.0	2.3	2.0
g116313.00860_ASC_T-10	1.5	0.75	9.0	5.0	3.6
g116313.00860_ASC_T-11	1.75	0.75	10.0	6.8	4.3
g116313.00860_ASC_T-12	2.0	0.75	10.0	8.1	4.9
g116313.00860_ASC_T-13	0.75	1.0	6.5	0.9	0.8
g116313.00860_ASC_T-14	1.0	1.0	7.0	1.8	1.4
g116313.00860_ASC_T-15	1.25	1.0	8.0	2.9	1.9
g116313.00860_ASC_T-16	1.5	1.0	9.0	4.3	2.4
g116313.00860_ASC_T-17	1.75	1.0	10.0	6.1	3.0
g116313.00860_ASC_T-18	2.0	1.0	10.0	7.2	3.4

Table 4.1.2.2*: Parameters of the ASC scan at elongation of 2.42 and triangularities of 0.66. The height of the inner strikepoint is Z=-1.39 in these equilibria.*

Once again, very large heat fluxes are observed, especially in the scan at elongation of 2.3 in Table 4.1.2.1. At higher elongation, reflected in Table 4.1.2.2, where the PF-1a current can be dropped, the heat fluxes are somewhat reduced, primarily through poloidal flux expansion. This has the consequence of reducing the minimum angle of attack, requiring more precise alignment of PFCs. To establish long-pulse operations at the higher elongations will require demonstrating operations at lower elongation, so cases in Table 4.1.2.1 are still relevant, but at shorter durations.

4.2: Lower Single Null Cases

Lower single null (LSN) equilibria have a dominant X-point on the lower portion of the plasma boundary. These will typically have significantly higher heat fluxes on the lower vertical target, due to power that can flow over the top of the plasma and down the inboard side to the inner strike-point. For strongly lower single cases, $dr_{sep}/\lambda_q >> 1$, the model assumes that 30% of the input power is going to the inner target, with 70% going to the outer. In contrast, in DN plasmas the model assumes only 10% of the power is going to the lower, inner target. LSN cases were requested from the DivSOL [3], PED [5], and MPFC TSGs [8].

4.2.1: LSN Cases from the Div-SOL Research Agenda

Quantity	Units	Value
elongation	---	2.2

lower triangularity	---	0.65
upper triangularity	---	0.3
dr_{sep}	cm	-0.6
Z_{ISP}	m	-1.34

Table 4.2.1.1*: Common parameters for the LSN scans in this section*

These DivSOL studies here were typically based on 2-3 nearby equilibria for each configuration. These equilibria had some small planned variation in the outer strikepoint radius, but very small variation in the inner strike-point height. An example set of equilibria is shown in Fig. 4.2.1.1.

An example heat flux profile is shown in Fig. 4.2.1.2. The various colors correspond to:

- **green dashed:** averaged heat flux over the (small) sweep
- **red dot-dashed:** peak heat flux encountered at each location during the sweep
- **black solid:** heat flux profile for the single equilibrium

The peak heat flux for the single equilibrium under consideration is ~20 MW/m^2, which is quite close to the ~22 MW/m^2 flux of the most peaked profile in the very small scan.

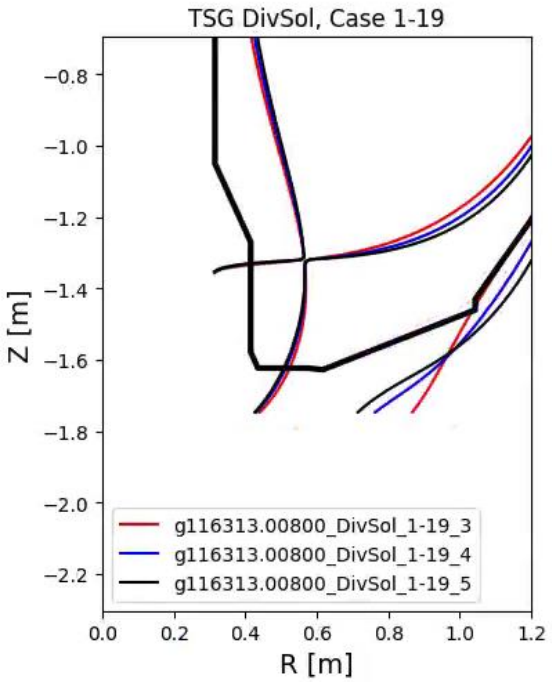

Fig. 4.2.1.1*: Example family of equilibria for one of the dr_{sep}=-6mm cases.*

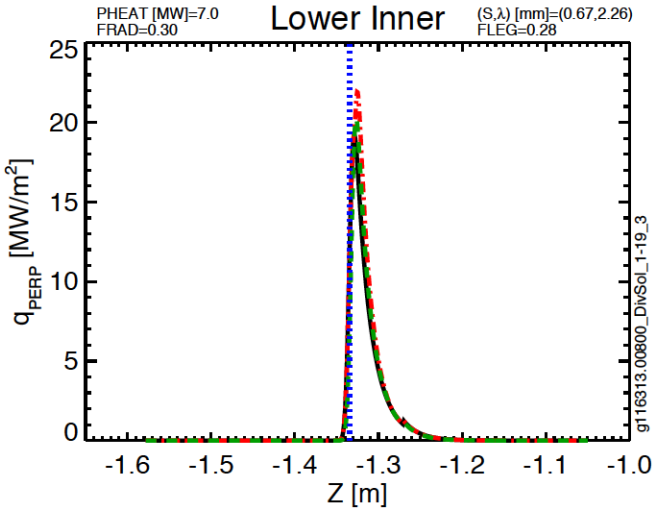

Fig. 4.2.1.2*: Heat flux profile on the inner target for the scan DivSOL, 1-19.*

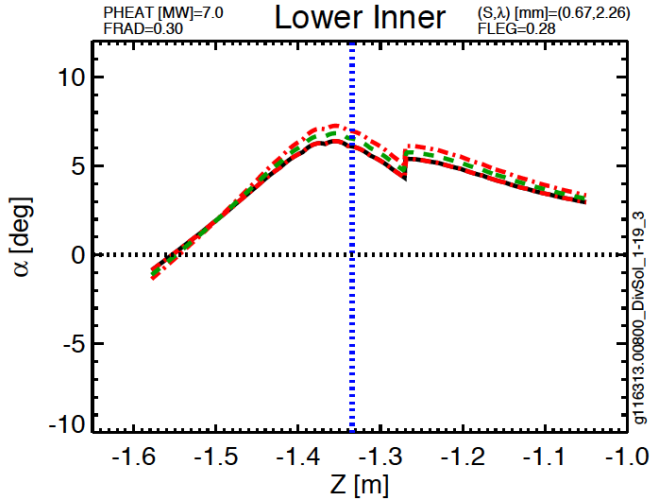

Fig. 4.2.1.3*: Field line angles on the inner vertical target for the scan DivSOL, 1-19.*

The profile of the field line angle is shown in Fig. 4.2.1.2. The field line angle is approximately 6.5 degrees at the peak of the heat flux profile. The discontinuity at Z ~ -1.34 [m] is the transition between the IBDV and the CSAS.

These types of calculations are repeated for the full set of equilibria, and are shown in Table. 4.2.1.2. Very high heat fluxes are observed at high current.

DivSOL Scenarios	**I_P**	**B_T**	**P_{inj}**	**q_{peak}**	**Angle at Peak**	**% to Inner Divertor**
	MA	**T**	**MW**	**MW/m^2**	**degrees**	**---**
1-13	0.5	0.5	3.0	1.5	2.8	0.21
1-14	1.0	0.5	4.0	7.4	6.7	0.26

1-17	0.5	0.75	3.0	1.4	1.6	0.22
1-18	1.0	0.75	5.0	8.3	3.7	0.26
1-19	1.5	0.75	7.0	22	6.1	0.28
1-21	0.5	1.0	4.0	1.5	1.1	0.23
1-22	1.0	1.0	7.0	10	2.5	0.27
1-23	1.5	1.0	9.0	26	4.7	0.28
1-24	2.0	1.0	10.0	43	6.0	0.29

Table 4.2.1.2*: Heat flux parameters on the vertical target for the scans LSN scans noted in Table 4.2.1.1. The percentage to lower IBDV is < 30% since* dr_{sep} *can be of order the heat flux width.*

From this table, it is clear that unmitigated heat fluxes in some LSN configurations are likely to be beyond allowables for the most advanced PFC designs, even when considering the TSG request of durations of 1-2 seconds. Further heat flux mitigation through increased radiation is possible and in fact is a primary research focus for these targets. Additionally there is a large uncertainty in these predictions for the inner divertor heat flux width scaling. Thus, while Scenarios like 1-23 and 1-24, and equivalents at higher I_p, should not drive PFC *heat flux* requirements, they represent a usage scenario for which the compatibility should be evaluated based on delivered IBDV designs and results from initial commissioning. In particular, due to PFC shaping, the *angle* requirements for these may still need to be considered in design requirements, since even if 85% of the power to the inner target could be removed for Scenario 1-24, dropping $q_{peak} \sim 6.3$ MW/m^2, if shaped tiles are not engineered to accept power flux at $\alpha \sim 6.5^o$, the case could remain incompatible with final IBDV designs.

4.2.2: LSN Cases from the Pedestal Research Agenda

The PED TSG [5] requested a series of equilibria at modest triangularity, in both double null and biased down with dr_{sep}*=-1.5 cm,* which is much larger than the assumed heat flux width. The DN cases will not challenge the PFCs compared to the LSN cases, and therefore only the LSN cases are considered here. There are similar results and implications as discussed in Section 4.2.1 as these scenarios have inner divertor heat flux far beyond expected IBDV capabilities.

I_P [MA]	1.2	B_T [T]	0.65	Δt [sec]	< 2.0
PED Scenarios	lower triangularity	Z_{Peak}	$P_{inj}+P_{HHFW}$	q_{peak}	Angle at Peak
	---	m	MW	MW/m^2	degrees
1-05	0.42	-1.4	6.0	18	7.1
1-06	0.51	-1.36	6.0	17	7.0

1-17	0.42	-1.41	10.0	28	7.1
1-18	0.51	-1.37	10.0	28	7.0

Table 4.2.2.1*: Heat flux parameters on the vertical target for LSN scans at 1.2 MA and 0.65 T.*

I_P [MA]	1.4	B_T [T]	1	Δt [sec]	< 2.0
PED Scenarios	lower triangularity	Z_{ISP}	$P_{inj}+P_{HHFW}$	q_{peak}	Angle at Peak
	---	m	MW	MW/m^2	degrees
2-04	0.36	-1.45	8.0	19	3.8
2-05	0.44	-1.41	8.0	28	5.7
2-06	0.52	-1.37	8.0	27	5.5

Table 4.2.2.2*: Heat flux parameters on the vertical target for LSN scans at 1.4 MA and 8 MW.*

I_P [MA]	1.8	B_T [T]	1	Δt [sec]	< 2.0
PED Scenarios	lower triangularity	Z_{ISP}	$P_{inj}+P_{HHFW}$	q_{peak}	Angle at Peak
	---	m	MW	MW/m^2	degrees
2-16	0.35	-1.46	10.0	37	5.8
2-17	0.43	-1.40	10.0	50	7.8
2-18	0.51	-1.37	10.0	48	7.5

Table 4.2.2.3: *Heat flux parameters on the vertical target for LSN scans at 1.8 MA and 10 MW.*

4.3: Summary of Vertical Target Heat Fluxes for Stationary H-modes

The data in Sections 4.1 and 4.2 is combined in Figure 4.3.1 and Figure 4.3.2. The first figure shows the peak heat flux as a function of plasma current for the PED, ASC and DivSOL TSG scans. Double null cases can exceed 8 MW/m^2, while high current LSN cases can approach 40 MW/m^2. These are larger than the expected allowables for PFCs based on isotropic graphite, and therefore some method of heat flux reduction (e.g. strikepoint sweeping or enhanced radiation from impurity seeding) would be necessary. As previously mentioned, compatibility would be judged based on delivered IBDV designs and results from initial plasma commissioning.

Note that at I_P=2 MA, midplane scrape-off layer widths are typically of order 2 mm, and therefore controllability of dr_{sep} on this scale is important in avoiding LSN/USN-level heat fluxes in nominal DN scenarios. If these dr_{sep} variations are oscillatory, their effect may average out, although the upper IBDV would see higher heat flux than the lower in cases that are slightly biased USN due to ExB drift asymmetries. Thus large, steady-state

dr_{sep} errors scale need to be eliminated to prevent unintended heat loading of the vertical target at single null levels.

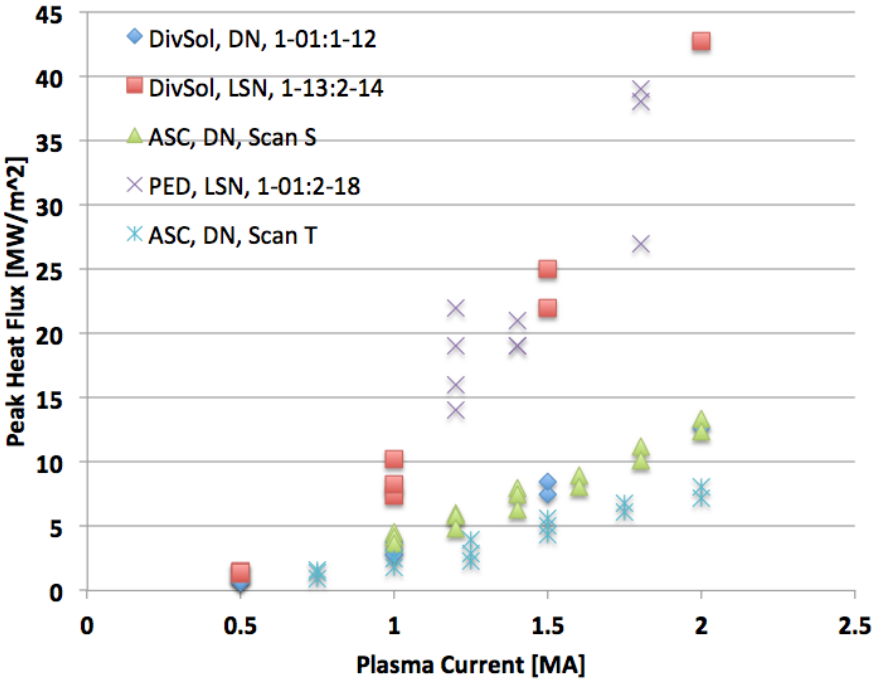

Fig. 4.3.1*: Peak heat fluxes for cases in Section 4, as a function of plasma current.*

Field line angles are shown in Fig. 4.3.2. Angles range from just below 1 degree to above 8 degrees. The present requirements in Table 2.1 have a maximum angle of 6.0 degrees, making it likely that a few of these cases will not be compatible with the final designs of shaped PFCs.

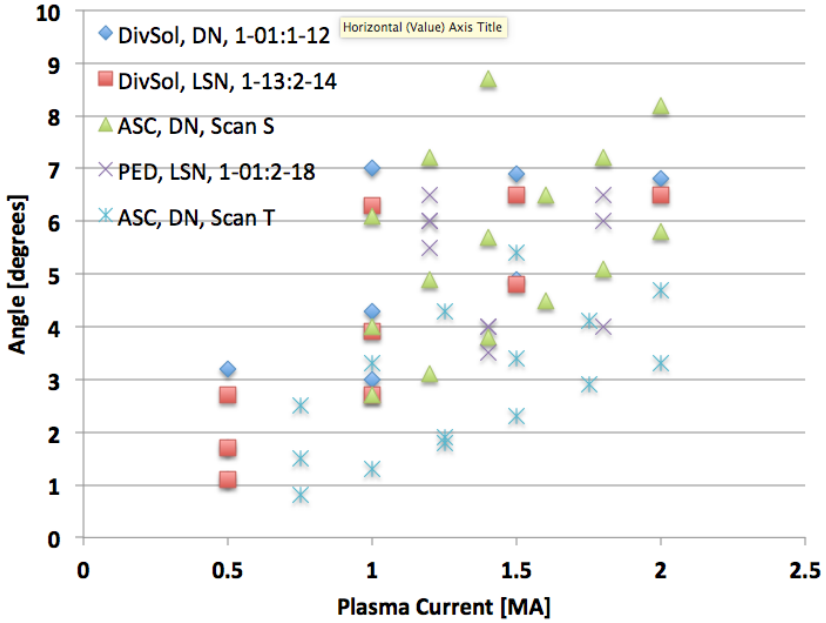

Fig. 4.3.2*: Field line angle at the location of peak heat flux versus I_p for cases in Section 4*

5: LSN H-Mode Sweeps on the IBDV

The previous section showed that large heat fluxes can be found on the inner target, likely exceeded PFC heat flux handling limits even in double-null if that leg remains in an "attached" state. To mitigate the large heat fluxes on the inner vertical target, sweeping has been considered. This section considers results from studies to vertically sweep the inner strikepoint.

Multiple sweeping strategies were developed and the relative advantages to each would depend on the nature of the experiment under consideration:

- Sweep the inner strikepoint via adjustments to the X-point(s). In LSN plasmas, this can be done by shifting the plasma up and down.
- Sweep with fixed X-point(s) using variations in the shape parameters, such outer squareness and inner gap.
- Combinations of these strategies are also possible.

In any sweeping case, further plasma control work is required to develop these techniques, as well as operations time during NSTX-U commissioning to demonstrate them. The Tables 5.1-5.4 and Figure 5.1-5.8 illustrate scans that form the basis for requirements in Table 2.1, while all scans considered are shown in the Appendix.

Scan DivSol 8-05	Common Scan Quantity	Value
g116313.008600_DivSol_8-05_1	I_P [MA]	1.8
g116313.008600_DivSol_8-05_5	B_T [T]	1
g116313.008600_DivSol_8-05_7	P_{inj} [MW]	10
g116313.008600_DivSol_8-05_8	betaN	4
g116313.008600_DivSol_8-05_11	dr_{sep} [cm]	-1
g116313.008600_DivSol_8-05_10	Typical Lower Triangularity	0.4

***Table 5.1**: Parameters for DivSOL scan 8-05.*

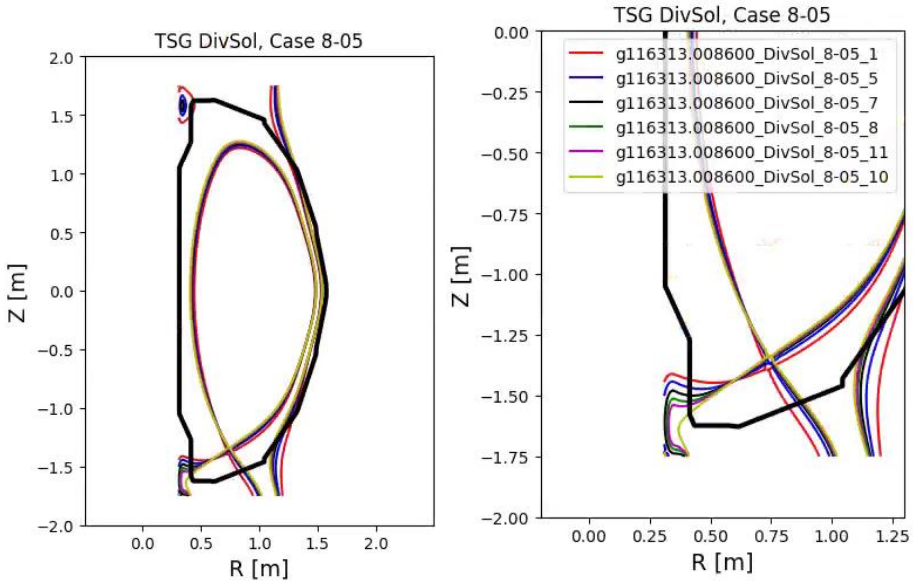

***Fig. 5.1**: Equilibria for scan DivSOL, 8-05*

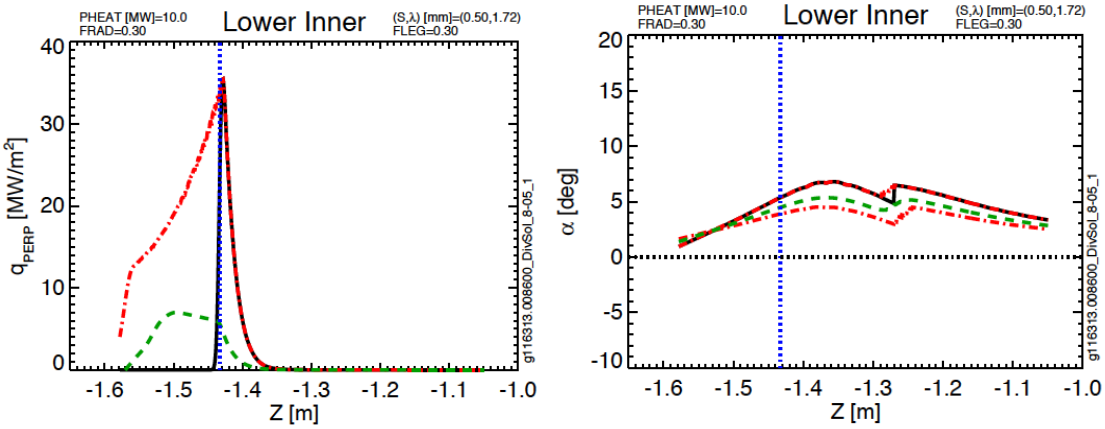

***Fig 5.2**: Lower inner target parameters from DivSOL Scan 8-05*

Scan PED, 2-05	Common Scan Quantity	Value
g116313.00800_PED_2-05_1	I_P [MA]	1.4
g116313.00800_PED_2-05_2	B_T [T]	1
g116313.00800_PED_2-05_3	P_{inj} [MW]	8
g116313.00800_PED_2-05_4	dr_{sep} [cm]	-1.5
g116313.00800_PED_2-05_5	Typical Lower Triangularity	0.45

***Table 5.2**:Parameters for PED scan 2-05.*

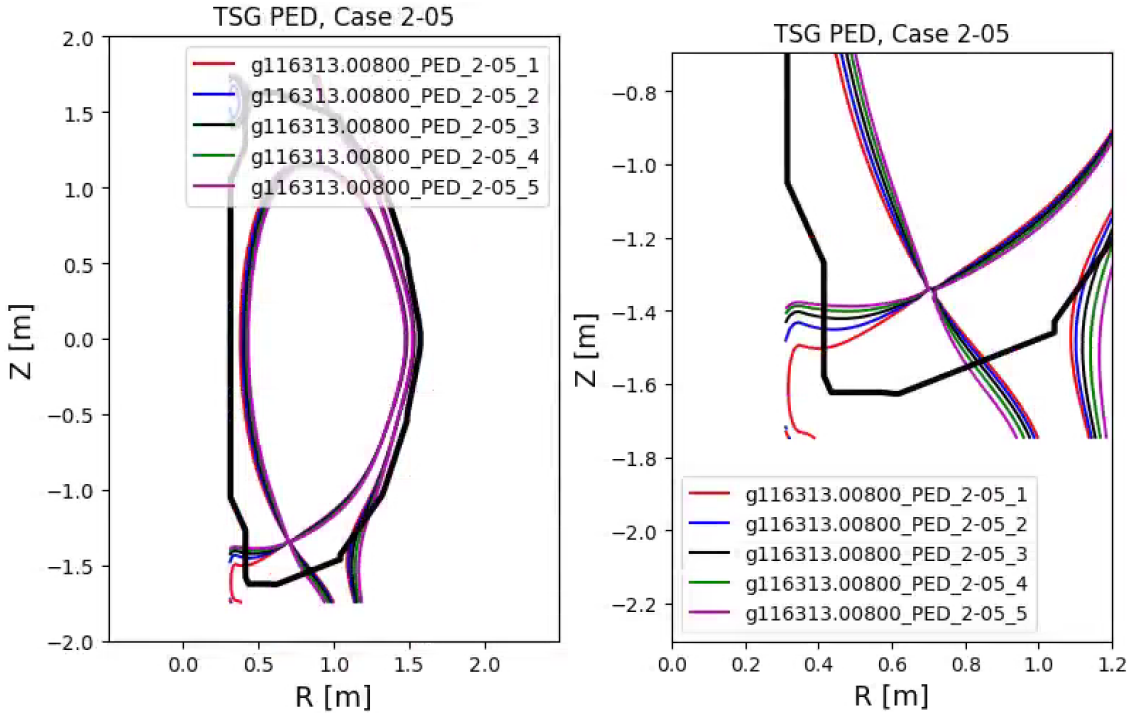

***Fig. 5.3**: Equilibria for scan PED, 2-05*

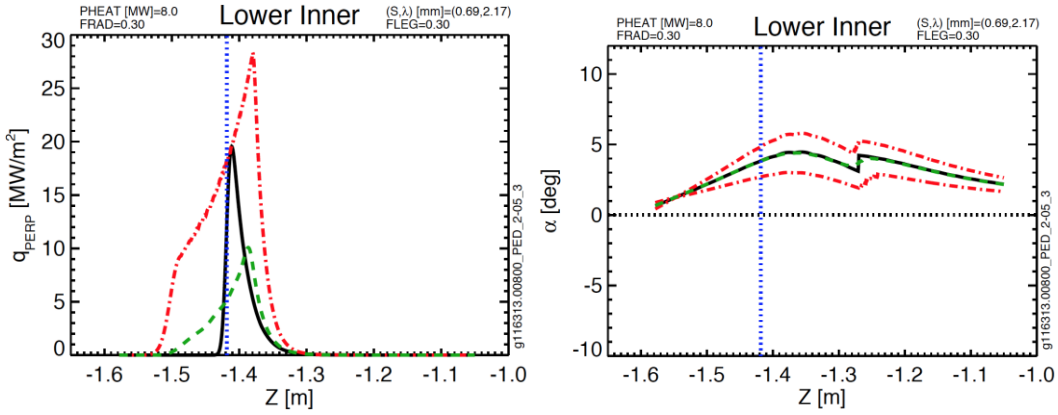

***Fig. 5.4**: Lower inner target parameters for PED 2-05*

Case 2, Scan 4	Common Scan Quantity	Value
g135111.00500_k2.55_d0.70_z0.04	I_P [MA]	2
g135111.00500_k2.53_d0.70_z0.08	B_T [T]	1
g135111.00500_k2.51_d0.70_z0.10	P_{inj} [MW]	10
g135111.00500_k2.49_d0.70_z0.11	dr_{sep} [cm]	0
g135111.00500_k2.47_d0.70_z0.20	Typical Elongation	2.5
g135111.00500_k2.45_d0.70_z0.27	Typical Lower Triangularity	0.7

***Table 5.3**: Parameters for Case 2, Scan 4.*

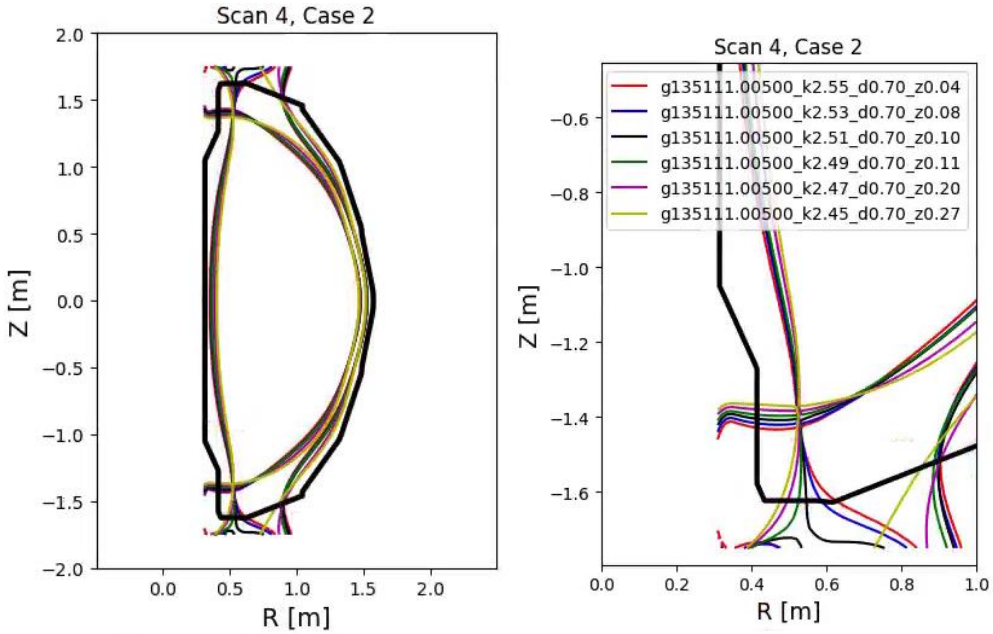

***Fig. 5.5**: Equilibria for Case 2, Scan 4.*

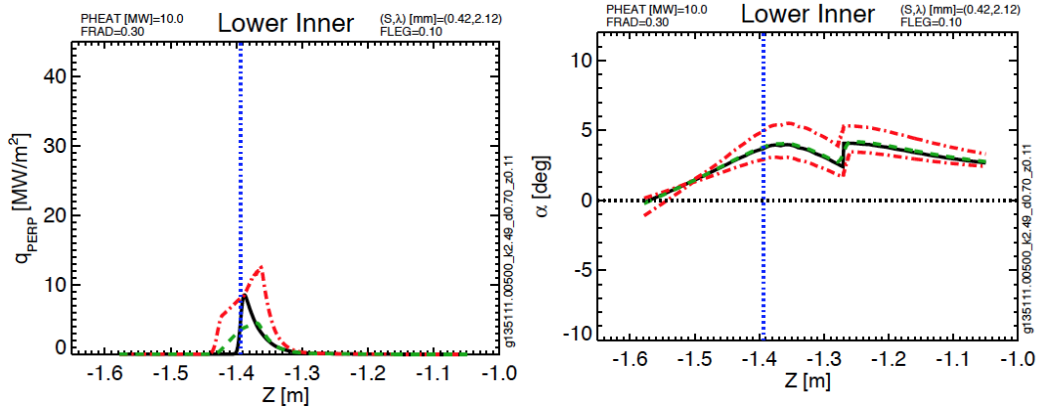

***Fig. 5.6**: Lower inner target parameters for Case 2, Scan 4*

Case 3, Scan 1	Common Scan Quantity	Value
g135111.00500_k2.55_d0.70_z0.06	I_P [MA]	2
g135111.00500_k2.53_d0.70_z0.07	B_T [T]	1
g135111.00500_k2.51_d0.70_z0.08	P_{inj} [MW]	10
g135111.00500_k2.49_d0.70_z0.12	dr_{sep} [cm]	0
g135111.00500_k2.47_d0.70_z0.17	Typical Elongation	2.5
g135111.00500_k2.45_d0.70_z0.27	Typical Lower Triangularity	0.7

***Table 5.4**: Parameters for Case 3, Scan 1.*

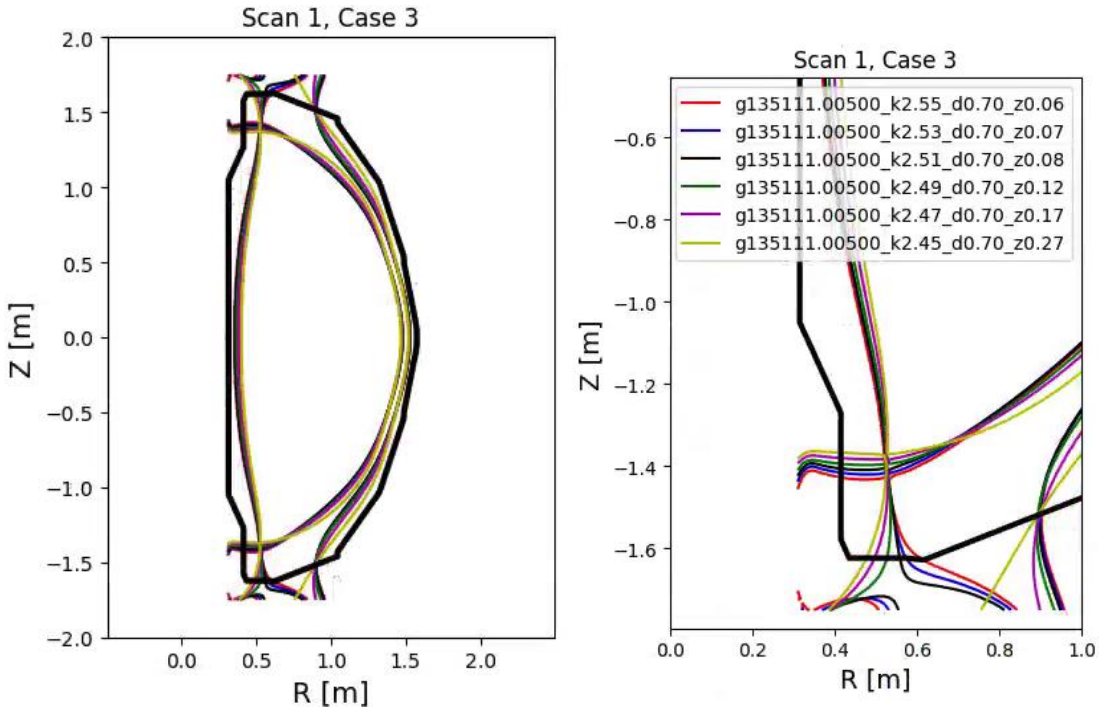

***Fig. 5.7**: Equilibria for Case 3, Scan 1.*

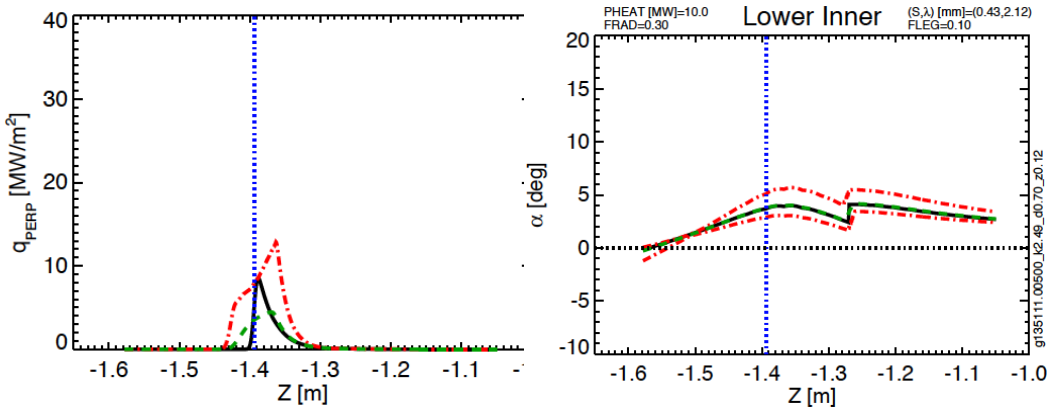

***Fig. 5.8**: Lower inner target parameters for Case 3, Scan 1*

Scan	[I_P,B_T,P_{heat}]	dr_{sep}	Vertical Range of ISP Sweep	Peak Instantaneous Heat Flux	Peak Swept Heat Flux	Angle Range at Z_{min}	Angle Range at Z_{max}
---	[MA,T,MW]	cm	m	MW/m^2	MW/m^2	degrees	degrees
DivSol, 8-01	[2, 1, 10]	-0.6	[-1.37, -1.29]	49	12	5.7	6.8
DivSol, 8-02	[2, 1, 10]	-0.6	[-1.41, -1.36]	67	17	7.6	9.8
DivSol, 8-03	[1, 1. 8]	-0.6	[-1.38, -1.35]	21	17	4.4	4.6
DivSol, 8-04	[1, 1, 7]	-1	[-1.56, -1.48]	8.3	5.6	1.0	1.9
DivSol, 8-05	**[1.8, 1, 10]**	**-1**	**[-1.57, -1.43]**	**35**	**7.0**	**1.7**	**5.3**
DivSol, 8-06	[1.8, 1, 10]	-1	[-1.5, -1.44]	36	16	2.6	5.5
DivSol, 8-07	[1, 1, 7]	-1	[-1.56, -1.48]	9.6	6.4	0.75	2.3
Ped, 1-05	[1.2, 0.65, 6]	-1.5	[-1.44, -1.39]	18	9.1	3.6	7.0
Ped, 1-17	[1.2, 0.65, 10]	-1.5	[-1.44, -1.39]	28	15	3.6	7.0
Ped, 2-04	[1.4,1.8]	-1.5	[-1.50, -1.45]	19	11	2.3	3.6
Ped, 2-05	**[1.4, 1, 8]**	**-1.5**	**[-1.5, -1.38]**	**28**	**10**	**1.7**	**5.6**
Ped, 2-16	[1.8, 1, 10]	-1.5	[-1.53, -1.43]	37	11	2.2	5.6
MPFC, 2-01	[1.25, 0.76, 3]	-1.5	[-1.4, -1.37]	9.0	6.5	5.3	5.5
MPFC, 3-02	[700,0.7,2]	-1.6	[-1.37, -1.32]	5.4	2.9	5.7	5.9

Table 5.5*: Vertical target heat flux parameters and angles for various scans, in LSN scenarios.*

Scan	[I_P,B_T,P_{heat}]	dr_{sep}	Vertical Range of ISP Sweep	Peak Instantaneous Heat Flux	Peak Swept Heat Flux	Angle Range at Z_{min}	Angle Range at Z_{max}
---	[MA,T,MW]	cm	m	MW/m^2	MW/m^2	degrees	degrees
Case 1, Scan 7	[2, 1, 10]	0	[-1.36, -1.32]	23	8.6	9.8	7.2
Case 1, Scan 8	[2, 1, 10]	0	[-1.40, -1.35]	18	8.9	7.2	7.0
Case 2, Scan 4	**[2, 1, 10]**	**0**	**[-1.43, -1.37]**	**12**	**4.5**	**2.5**	**5.4**
Case 2, Scan 5	[2, 1, 10]	0	[-1.47, -1.39]	11	3.9	1.8	4.5
Case 2, Scan 6	[2, 1, 10]	0	[-1.49, -1.43]	7.6	4.3	1.3	3.2
Case 3, Scan 1	**[2, 1, 10]**	**0**	**[-1.43, -1.37]**	**13**	**4.5**	**2.4**	**5.5**
Case 3, Scan 2	[2, 1, 10]	0	[-1.46, -1.39]	11	4.0	1.8	4.6
Case 4, Scan 1	[2, 1, 10]	0	[-1,44, -1.36]	12	4.1	2.3	5.3
Case 4, Scan 2	[2, 1, 10]	0	[-1.49, -1.40]	10	3.4	1.6	4.5
Case 4, Scan 3	[2, 1, 10]	0	[-1.53, -1.44]	7.4	3.4	1.3	3.1

Table 5.6*:Vertical target heat flux parameters and angles for various scans, in DN (dr_{sep}=0) scenarios.*

Tables 5.5 and 5.6 summarize LSN and DN sweeping scenarios which drive requirements for the IBDV PFCs. Note that the Case/Scan series in Table 5.6 is derived from inputs from the ASC TSG. There are multiple examples in Table 5.5 of scenarios that will only be compatible assuming significant reduction in inner target heat flux through radiation. To obtain operational space for these DivSOL and PED TSGs, the Case#2 requirement is set in Table 2.1 for the IBDV to allow short, ~1 second, pulses of up to 10 MW/m^2 for angles up to 6.0 degrees. A lower angle limit, to test edge loading/shadowing conditions is set to 2.0 degrees. Note that the scans, as shown in Figures 5.2 and 5.4 indicate that at the lower angles of incidence the power flux will be reduced, so testing 10 MW/m^2 at 2.0 degrees may be overly conservative.

From Table 5.6, the long, ~5 second, pulse at high current, field and power cases in DN are listed, and it is critical that a number of these options are compatible with the IBDV design to insure a flexible operating space. All of the Case 2, 3 and 4 scans listed can be covered by the Case#1 requirement in Table 2.1 for operating at 5.0 MW/m^2 for angles up to 5.5 degrees. This is greater than the maximum peak swept power for those scans, in order to be conservative, since these represent compatibility of the 2 MA, 1 T, 10 MW cases of high importance to the NSTX-U mission. A lower angle limit, to test edge loading/shadowing conditions is set to 2.0 degrees, for the reasons previously described. This Case#1 requirement also satisfies MPFC requests in Table 5.5 that would be for long-pulse.

6: Stationary Cases with Large Poloidal Flux Expansion on IBDH and Compatibility with Snowflake Divertors

It is possible to produce cases of large poloidal flux expansion on the horizontal target, allowing stationary operation at high current, field and power for the outer strikepoint. The compatibility of the inner strike point for these configurations will be discussed in a future revision to this memo. They are discussed for the IBDH in Section 5 of [2].

The inboard divertor vertical target tiles shall accept the stationary reversed helicity heat flux as per Table 6.1. This is included in Table 2.1 as requirement Case #4 and comes from a need to handle power on the reversed leg of a snowflake divertor for DivSOL research [3]. Note that there is not a validated means to project the power that will flow into the inner legs of a snowflake divertor, and therefore, this heat flux estimate has larger than normal uncertainty.

Case Index	Geqdsk file	Average Heat Flux	Duration	|Inclination Angle|
---	---	MW/m^2	s	degrees
NA	NA	1	1	1-5

Table 6.1*: Heat flux characteristics cases on the inboard divertor horizontal surface for the reversed helicity case.*

7: General Dependencies on the X-Point Height

The studies in this report show that there are a number of broad conclusions that can be drawn regarding dependency of the inner strikepoint along the vertical target. These are largely indicated in Fig. 7.1 where the field line angle at the strikepoint is shown as a function of height along the target. The data in this figure come from the following sources:

- The I_P=2 MA, B_T=1 T scenarios in the spreadsheet in [9].
- The I_P and B_T scans in Section 4.
- The two ends of each strikepoint scan in Tables 5.5 and 5.6. Note the later of these are all I_P=2 MA, B_T=1 T scenarios.

From this table, as well as inspection of the underlying data, it is clear that the primary heat flux handling surface on the lower IBDV starts above approximately Z=-1.5 m. A few cases have scans with the ISP beneath this level (DivSOL 8-05, DivSOL 8-07, PED 2-16), but these cases have low triangularity, and are expected to only operate for short pulses as per TSG requests. From this the Case#3 requirement is added to Table 2.1 that the regions |Z| > 1.5 m in the upper and lower divertor default back to the levels expected for 'modest improvements', 3.5 MW/m^2 for 5 seconds, employed elsewhere in NSTX-U, but with the expectation of more grazing angles of incidence, from 1.0-4.0 degrees.

The second observation is that for the I_P=2 MA, B_T=1 T case, there is a clear tendency for the field line angle to increase as the ISP moves up the target. Field line angles of 1-3 degrees would be appropriate around Z=-1.46, with angles of 3-6 appropriate around Z=-1.38. However, this trend is broken once additional values of I_P and B_T are included in the simulation. More detailed analysis could be completed if there is benefit to having the maximum field line angle discretized versus IBDV position in order to better optimize tile shaping. The Case#2 requirement in Table 2.1 should allow these configurations even if tile shaping is used, but may require enhanced radiation to drop heat fluxes to be within design limits. The addition of private flux region gas fueling is expect to facilitate this.

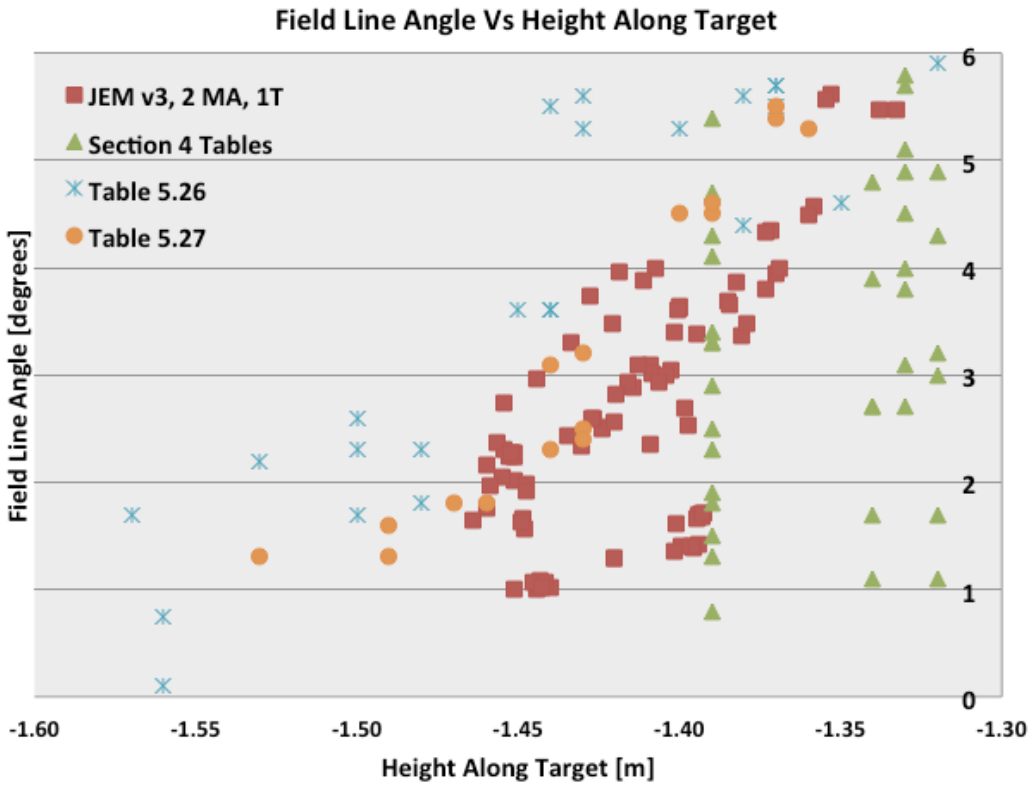

***Fig. 7.1**: Field line angles vs. height along the target. See text for more detail*

8: Strategies for Heat Flux Mitigation and Control

It is clear from this Sections 4-7 that many stationary and some sweeping heat fluxes on the IBDV can be prohibitively large requiring further mitigation and/or control. The flexibility to employ poloidal flux expansion on the IBDV is much more limited than the IBDH due to the PF1 coil locations, but options remain, some of which could be used in tandem:

- Use of radiation to dissipate the power, either through neutral interactions or impurity seeding. To this end, a requirement for private flux region gas fueling has been added to the PFC Requirements.
- Use of model-based power partitioning control using rtEFIT and other potential diagnostics, which can keep track of integrated energy flux input to various PFCs relative to design limits.
- Use of real-time monitoring of PFC surface temperature using IR/NIR thermography, linked to PCS which can initiate controlled shutdowns if temperature limits are reached.

Continued efforts, done in parallel with IBDV design, can assess which of these techniques may be most appropriate for NSTX-U. With sufficient resources and planning, they can be expected to be available in the post-Recovery commissioning phase, allowing the IBDV to support a robust science program once Research operations resumes.

References

[1] Memo PFCR-MEMO-008-00, *Heat Fluxes on the CSAS and Far OBD Regions*
[2] Memo PFCR-MEMO-010-00: *Heat Fluxes on the IBDH and OBD Row 1 and Row 2*
[3] Memo DivSol-170524-VS-02: *Impact of Polar Regions on DivSol Research*
[4] Memo ASC-170523-DB-02, *Impact of Proposed Polar Region Modifications on Research and Scenarios for ASC Topical Science Group*
[5] Memo PED-171805-AD-02: *Impact of Potential Polar Region Modifications on Research and Scenarios for TSG-PED*.
[6] Memo TT-170523-WG-01, *Impact of Potential Polar Region Modifications on Research and Scenarios for Transport and Turbulence Topical Science Group*
[7] Memo MS-170523-JN-04: *Impact of Potential Polar Region Modifications on Research and Scenarios for the Macroscope Stability Topical Science Group*
[8] Memo MPFC-170523-MJ-02: *Impact of Potential Polar Region Modifications on Research and Scenarios for the Material and Plasma Facing Components Topical Science Group*
[9] NSTX-U_simulation_results_combined_Menard_v3.xlsx

Appendix: Extended Tables and Plots of Sweeps

Tables and plots indicate the equilibria used in various sweeps and scans and the representative heat flux and field line angles.

DivSol, 1-01	**DivSol, 1-02**
g116313.00800_DivSol_1-01_4	g116313.00800_DivSol_1-02_3
g116313.00800_DivSol_1-01_5	g116313.00800_DivSol_1-02_4
	g116313.00800_DivSol_1-02_5
DivSol, 1-05	**DivSol, 1-06**
g116313.00800_DivSol_1-05_4	g116313.00800_DivSol_1-06_3
g116313.00800_DivSol_1-05_5	g116313.00800_DivSol_1-06_4
	g116313.00800_DivSol_1-06_5
DivSol, 1-07	**DivSol, 1-09**
g116313.00800_DivSol_1-07_3	g116313.00800_DivSol_1-09_4
g116313.00800_DivSol_1-07_4	g116313.00800_DivSol_1-09_5
g116313.00800_DivSol_1-07_5	
DivSol, 1-10	**DivSol, 1-11**
g116313.00800_DivSol_1-10_3	g116313.00800_DivSol_1-11_3
g116313.00800_DivSol_1-10_3	g116313.00800_DivSol_1-11_4
g116313.00800_DivSol_1-10_3	g116313.00800_DivSol_1-11_5
DivSol, 1-12	
g116313.00800_DivSol_1-12_2	
g116313.00800_DivSol_1-12_3	
g116313.00800_DivSol_1-12_4	
g116313.00800_DivSol_1-12_5	

Table A.1*: Equilibria used to make table 4.1.1.2*

DivSol, 1-13	DivSol, 1-14
g116313.00800_DivSol_1-13_3	g116313.00800_DivSol_1-14_3
g116313.00800_DivSol_1-13_4	g116313.00800_DivSol_1-14_4
g116313.00800_DivSol_1-13_5	g116313.00800_DivSol_1-14_5
DivSol, 1-17	**DivSol, 1-18**
g116313.00800_DivSol_1-17_4	g116313.00800_DivSol_1-18_3
g116313.00800_DivSol_1-17_5	g116313.00800_DivSol_1-18_4
	g116313.00800_DivSol_1-18_5
DivSol, 1-19	**DivSol, 1-21**
g116313.00800_DivSol_1-19_3	g116313.00800_DivSol_1-21_4
g116313.00800_DivSol_1-19_4	g116313.00800_DivSol_1-21_5
g116313.00800_DivSol_1-19_5	
DivSol, 1-22	**DivSol, 1-23**
g116313.00800_DivSol_1-22_3	g116313.00800_DivSol_1-23_4
g116313.00800_DivSol_1-22_4	g116313.00800_DivSol_1-23_5
g116313.00800_DivSol_1-22_5	
DivSol, 1-24	
g116313.00800_DivSol_1-24_3	
g116313.00800_DivSol_1-24_4	
g116313.00800_DivSol_1-24_5	

Table A.2*: Equilibria used to make table 4.2.1.2*

PED, 1-05	PED, 1-06
g116313.00800_PED_1-05_1	g116313.00800_PED_1-06_1
g116313.00800_PED_1-05_2	g116313.00800_PED_1-06_2
g116313.00800_PED_1-05_3	g116313.00800_PED_1-06_3
g116313.00800_PED_1-05_4	g116313.00800_PED_1-06_4
g116313.00800_PED_1-05_5	g116313.00800_PED_1-06_5
PED, 1-17	**PED, 1-18**
g116313.00800_PED_1-17_1	g116313.00800_PED_1-18_1
g116313.00800_PED_1-17_2	g116313.00800_PED_1-18_2
g116313.00800_PED_1-17_3	g116313.00800_PED_1-18_3
g116313.00800_PED_1-17_4	g116313.00800_PED_1-18_4
g116313.00800_PED_1-17_5	g116313.00800_PED_1-18_5
PED, 2-04	**PED, 2-05**
g116313.00800_PED_2-04_4	g116313.00800_PED_2-05_1
g116313.00800_PED_2-04_5	g116313.00800_PED_2-05_2
	g116313.00800_PED_2-05_3
	g116313.00800_PED_2-05_4
	g116313.00800_PED_2-05_5
PED, 2-06	**PED, 2-16**
g116313.00800_PED_2-06_1	g116313.00800_PED_2-16_3
g116313.00800_PED_2-06_2	g116313.00800_PED_2-16_4
g116313.00800_PED_2-06_3	g116313.00800_PED_2-16_5
g116313.00800_PED_2-06_4	
g116313.00800_PED_2-06_5	
PED, 2-17	**PED, 2-18**
g116313.00800_PED_2-17_1	g116313.00800_PED_2-18_1
g116313.00800_PED_2-17_2	g116313.00800_PED_2-18_2
g116313.00800_PED_2-17_3	g116313.00800_PED_2-18_3

g116313.00800_PED_2-17_4	g116313.00800_PED_2-18_4
g116313.00800_PED_2-17_5	g116313.00800_PED_2-18_5

Table A.3*: Equilibria used to make table 4.2.2.1, 4.2.2.2, and 4.2.2.3.*

Scan DivSol 8-01	Common Scan Quantity	Value
g204118.00600_DivSol_8-01_1	I_P [MA]	2
g204118.00600_DivSol_8-01_6	B_T [T]	1
g204118.00600_DivSol_8-01_4	P_{inj} [MW]	10
g204118.00600_DivSol_8-01_5	betaN	4
g204118.00600_DivSol_8-01_2	dr_{sep} [cm]	-0.6

Table A.4*: Parameters for DivSol scan 8-01.*

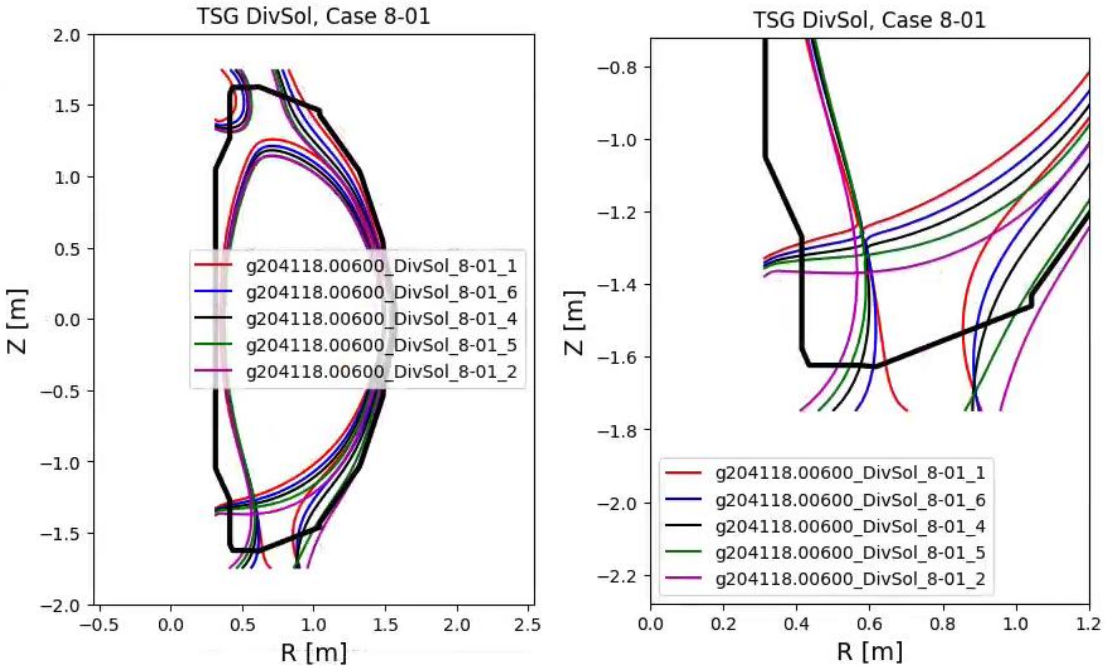

Fig. A.1*: Equilibria for scan DivSol, 8-01.*

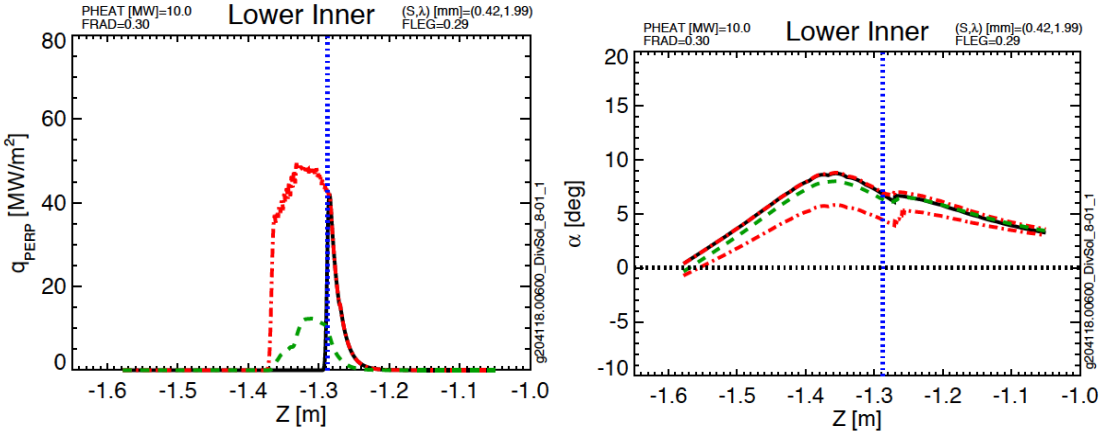

Fig A.2*: Lower inner target parameters from Scan 8-01*

Scan DivSol 8-02	Common Scan Quantity	Value
g204118.00600_DivSol_8-02_4	I_p [MA]	2
g204118.00600_DivSol_8-02_5	B_T [T]	1
g204118.00600_DivSol_8-02_2	P_{inj} [MW]	10
g204118.00600_DivSol_8-02_6	betaN	4
g204118.00600_DivSol_8-02_3	dr_{sep} [cm]	-0.6
g204118.00600_DivSol_8-02_7	Typical Lower Triangularity	0.5

***Table A.5**: Parameters for DivSol scan 8-02.*

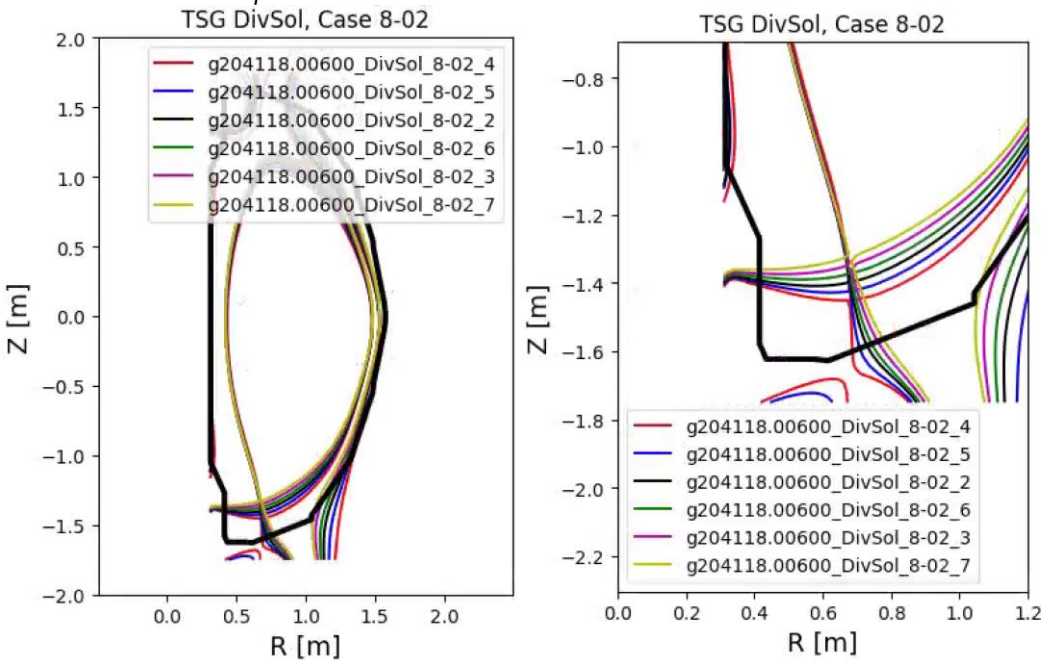

***Fig. A.3**: Equilibria for scan DivSol, 8-02.*

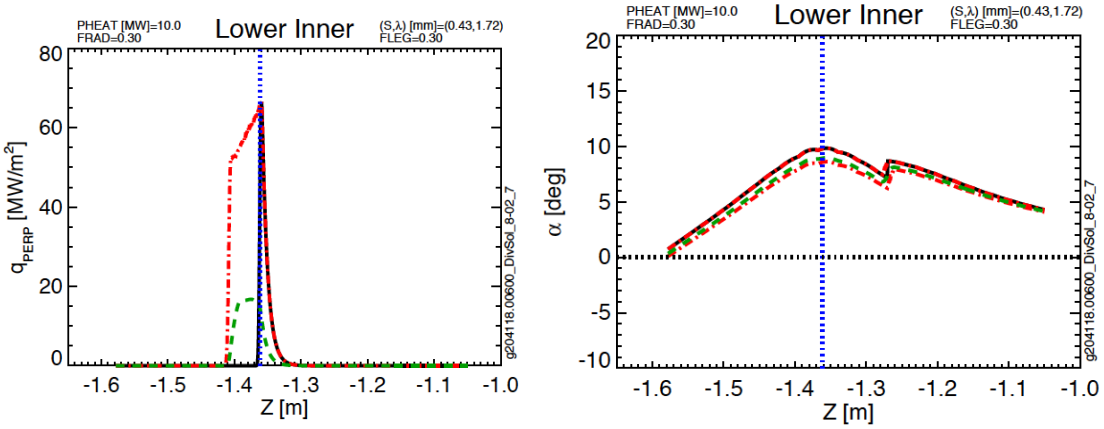

***Fig A.4**: Lower inner target parameters from Scan 8-02*

Scan DivSol 8-03	Common Scan Quantity	Value
g204118.00600_DivSol_8-03_1	I_P [MA]	1
g204118.00600_DivSol_8-03_6	B_T [T]	1
g204118.00600_DivSol_8-03_4	P_{inj} [MW]	8
g204118.00600_DivSol_8-03_5	betaN	4
g204118.00600_DivSol_8-03_3	dr_{sep} [cm]	-0.6

***Table A.6**: Parameters for DivSol scan 8-03.*

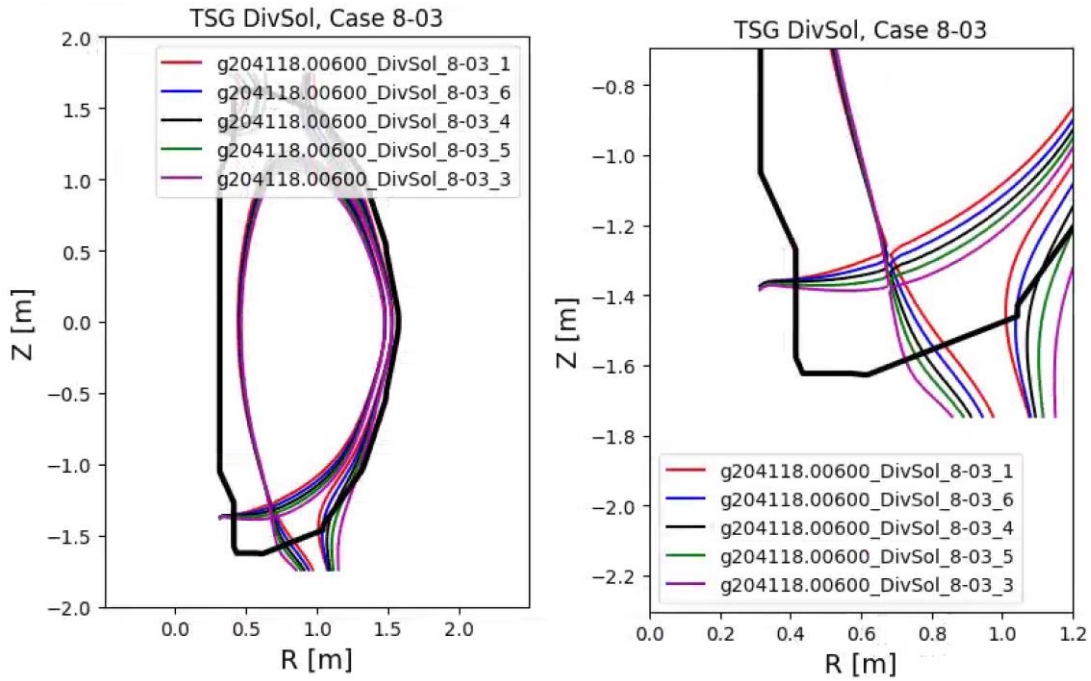

***Fig. A.5**: Equilibria for scan DivSol, 8-03.*

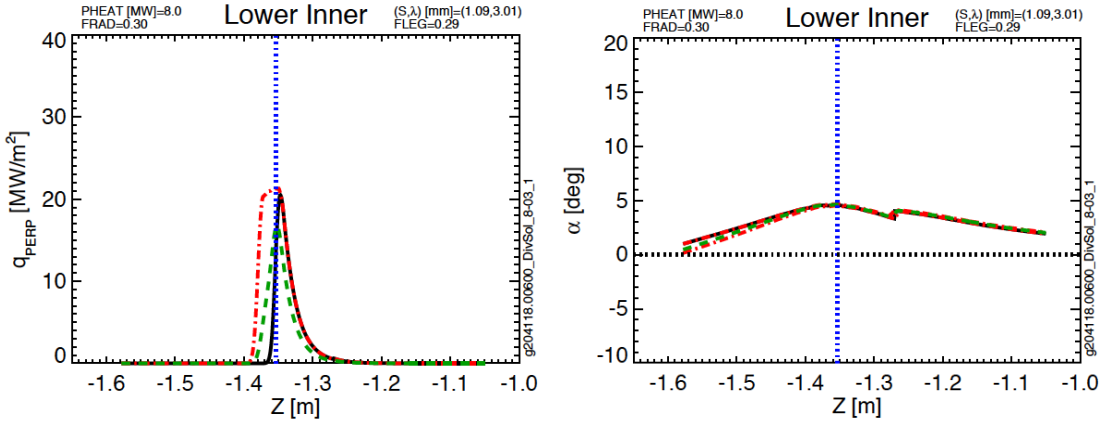

***Fig. A.6**: Lower inner target parameters from Scan 8-03.*

Scan DivSol 8-04	Common Scan Quantity	Value
g116313.008600_DivSol_8-04_5	I_P [MA]	1
g116313.008600_DivSol_8-04_6	B_T [T]	1
g116313.008600_DivSol_8-04_4	P_{inj} [MW]	7
g116313.008600_DivSol_8-04_3	betaN	4
g116313.008600_DivSol_8-04_1	dr_{sep} [cm]	-1
g116313.008600_DivSol_8-04_2	Typical Lower Triangularity	0.45

***Table A.7**: Parameters for DivSol scan 8-04.*

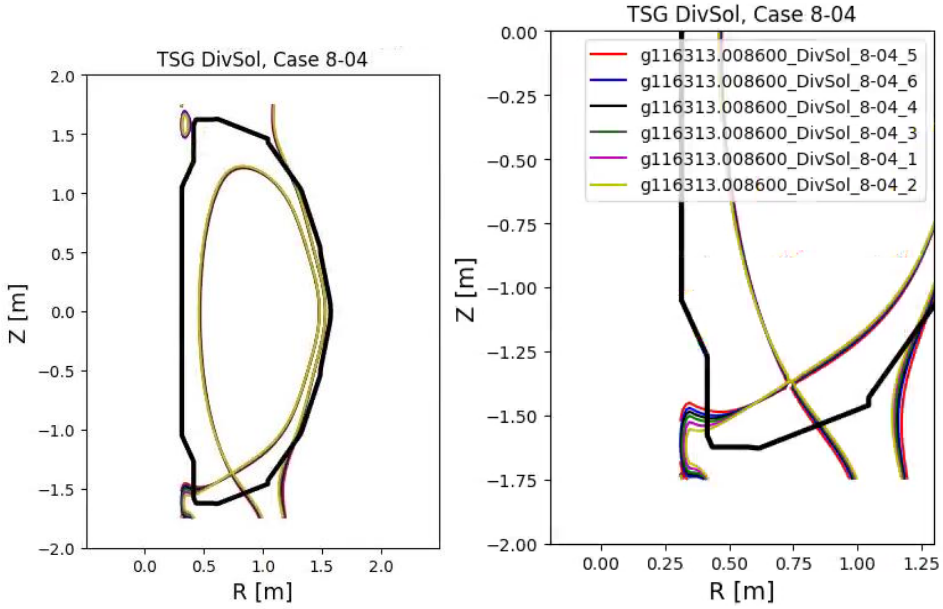

***Fig. A.7**: Equilibria for scan DivSol, 8-04.*

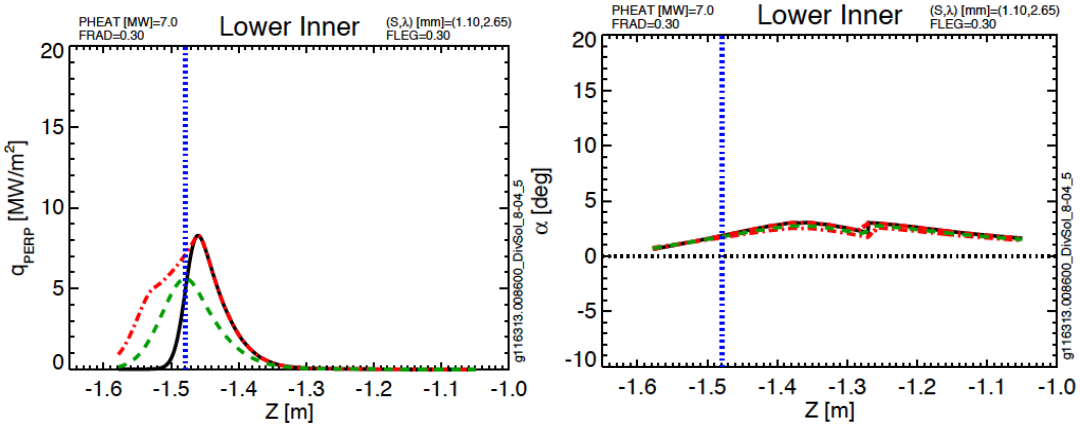

***Fig. A.8**: Lower inner target parameters from Scan 8-04*

Scan DivSol 8-05	Common Scan Quantity	Value
g116313.008600_DivSol_8-05_1	I_P [MA]	1.8
g116313.008600_DivSol_8-05_5	B_T [T]	1
g116313.008600_DivSol_8-05_7	P_{inj} [MW]	10
g116313.008600_DivSol_8-05_8	betaN	4
g116313.008600_DivSol_8-05_11	dr_{sep} [cm]	-1
g116313.008600_DivSol_8-05_10	Typical Lower Triangularity	0.4

***Table A.8**: Parameters for DivSol scan 8-05.*

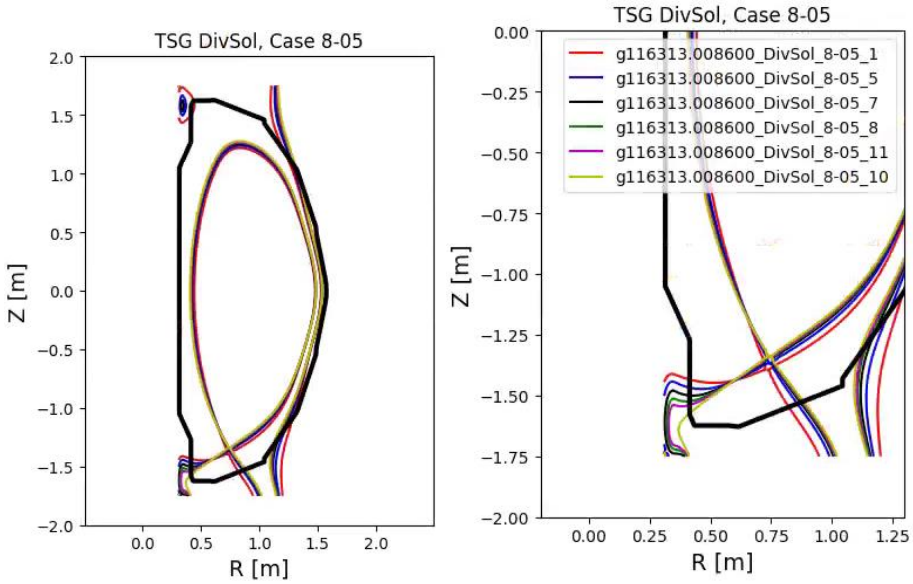

***Fig. A.9**: Equilibria for scan DivSol, 8-05.*

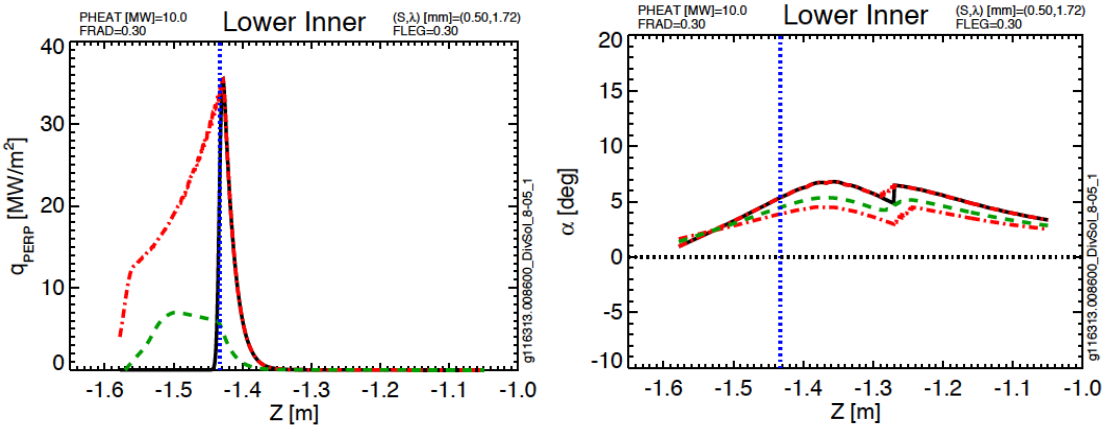

***Fig A.10**: Lower inner target parameters from Scan 8-05*

Scan DivSol 8-06	Common Scan Quantity	Value
g116313.008600_DivSol_8-06_5	I_P [MA]	1.8
g116313.008600_DivSol_8-06_1	B_T [T]	1
g116313.008600_DivSol_8-06_7	P_{inj} [MW]	10
g116313.008600_DivSol_8-06_2	betaN	4
g116313.008600_DivSol_8-06_6	dr_{sep} [cm]	-1
g116313.008600_DivSol_8-06_3	Typical Lower Triangularity	0.4

***Table A.9**: Parameters for DivSol scan 8-06.*

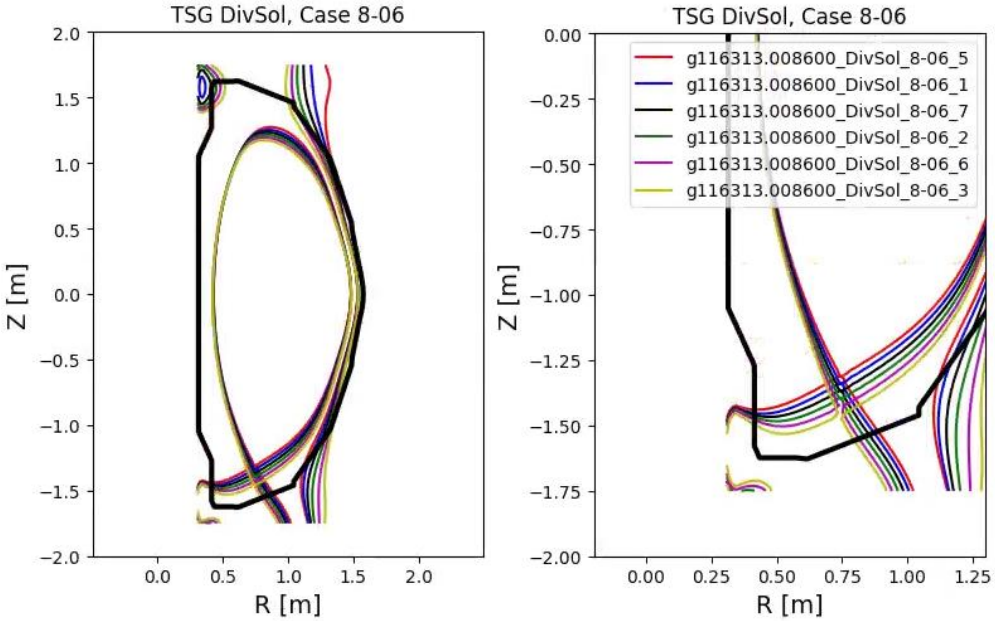

***Fig. A.11**: Equilibria for scan DivSol, 8-06.*

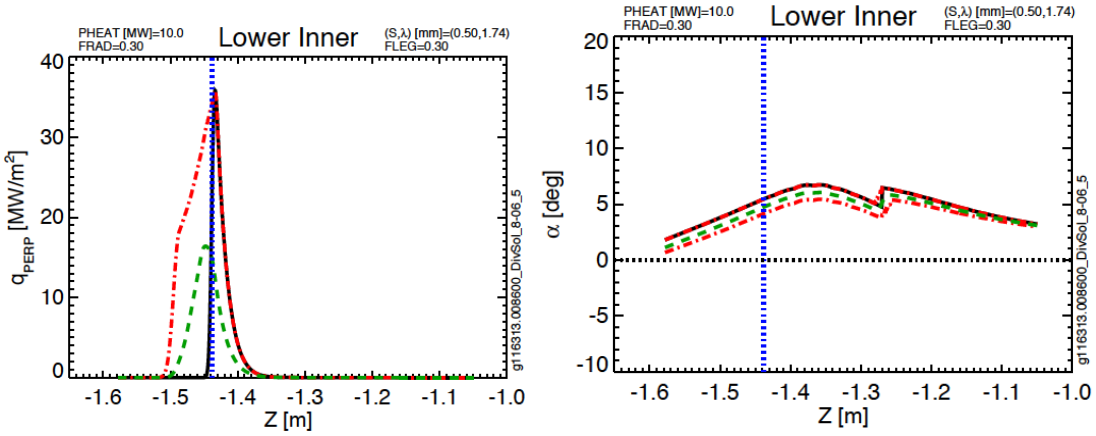

***Fig A.12**: Lower inner target parameters from Scan 8-06*

Scan DivSol 8-07	Common Scan Quantity	Value
g116313.008600_DivSol_8-07_6	I_P [MA]	1
g116313.008600_DivSol_8-07_5	B_T [T]	1
g116313.008600_DivSol_8-07_4	P_{inj} [MW]	7
g116313.008600_DivSol_8-07_1	betaN	4
g116313.008600_DivSol_8-07_2	dr_{sep} [cm]	-1

***Table A.10**: Parameters for DivSol scan 8-07.*

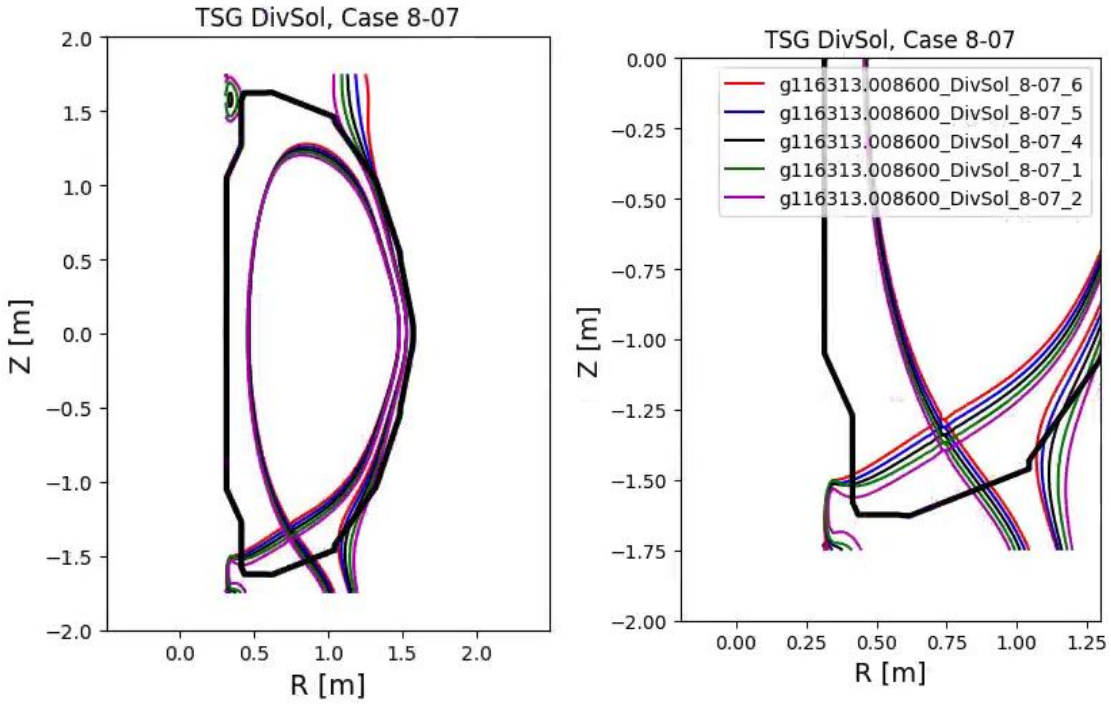

***Fig. A.13**: Equilibria for scan DivSol, 8-07.*

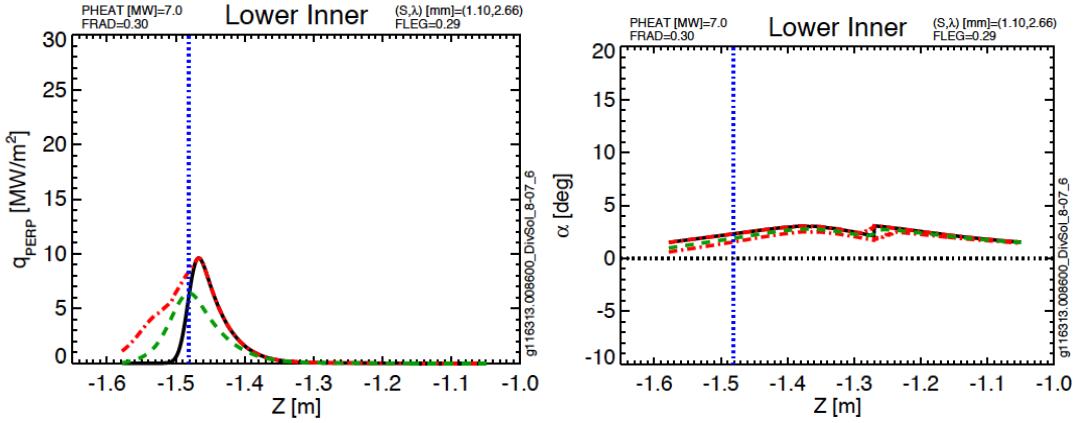

***Fig A.14**: Lower inner target parameters from Scan 8-07*

Scan PED, 1-05	Common Scan Quantity	Value
g116313.00800_PED_1-05_1	I_P [MA]	1.2
g116313.00800_PED_1-05_2	B_T [T]	0.65
g116313.00800_PED_1-05_3	P_{inj} [MW]	6
g116313.00800_PED_1-05_4	betaN	4
g116313.00800_PED_1-05_5	dr_{sep} [cm]	-1.5

***Table A.11**: Parameters for PED scan 1-05.*

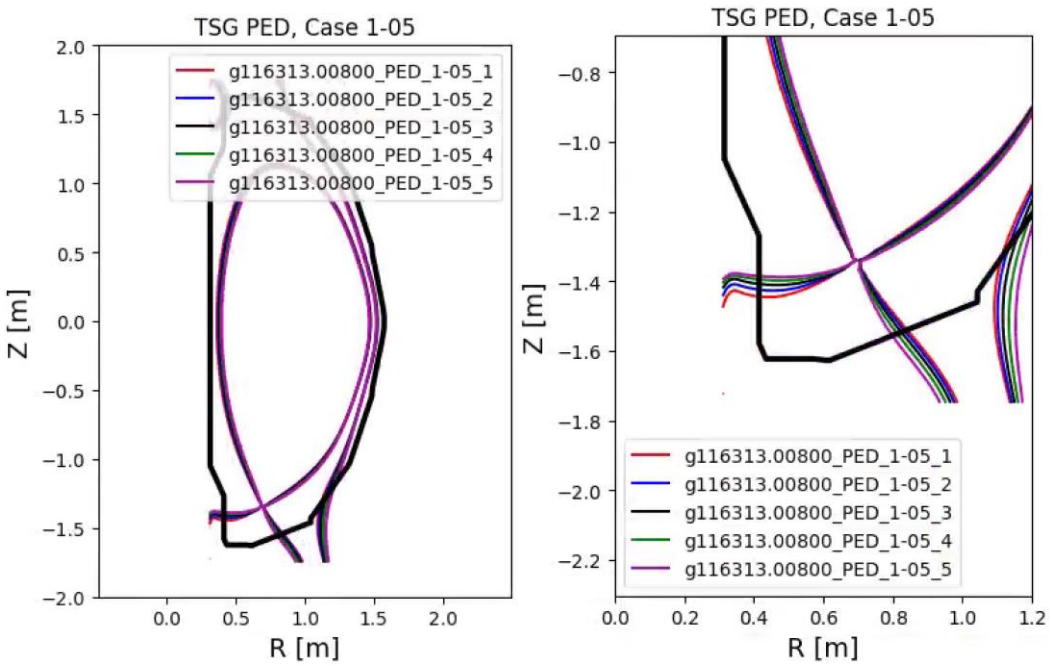

***Fig. A.15**: Equilibria for scan Ped, 1-05.*

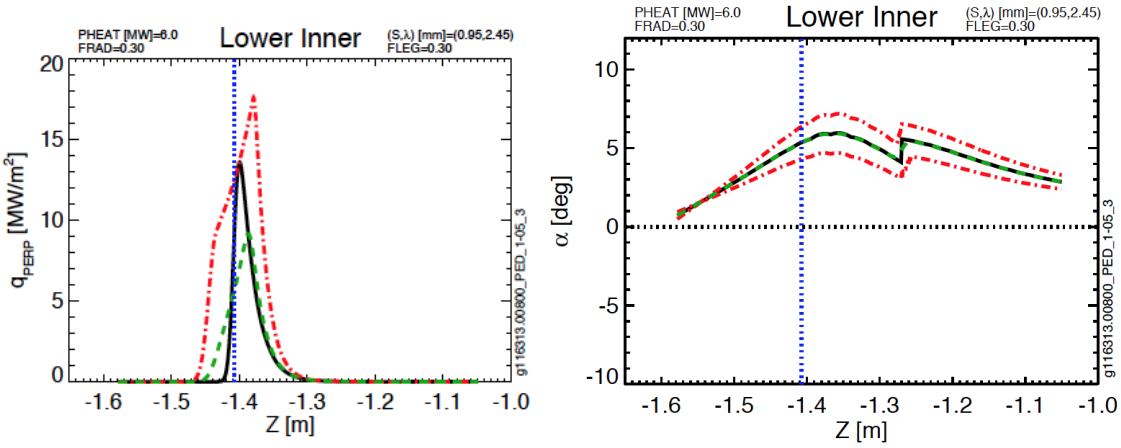

***Fig. A.16**: Lower inner target parameters for Ped 1-05*

Scan PED, 1-17	Common Scan Quantity	Value
g116313.00800_PED_1-17_1	I_P [MA]	1.2
g116313.00800_PED_1-17_2	B_T [T]	0.65
g116313.00800_PED_1-17_3	P_{inj} [MW]	10
g116313.00800_PED_1-17_4	betaN	4
g116313.00800_PED_1-17_5	dr_{sep} [cm]	-1.5
	Typical Lower Triangularity	0.437

***Table A.12**: Parameters for PED scan 1-17.*

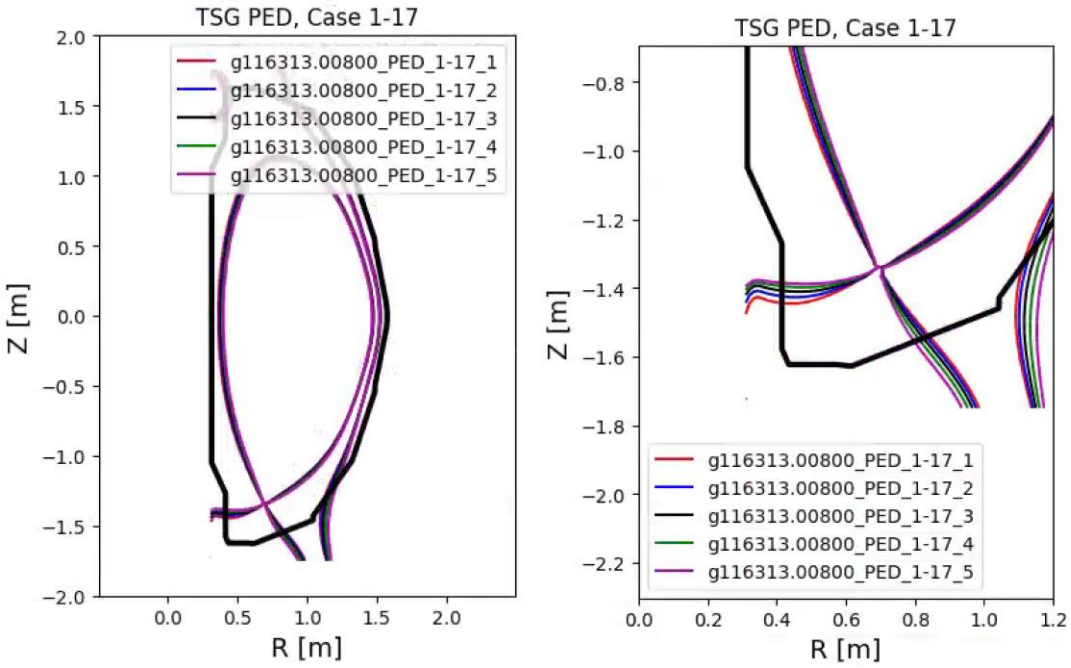

***Fig. A.17**: Equilibria for scan Ped, 1-17.*

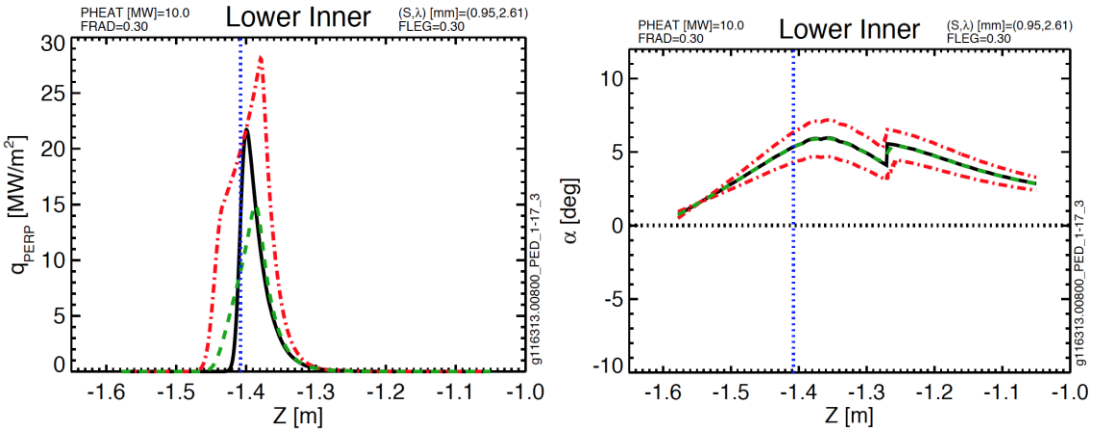

***Fig A.18**: Lower inner target parameters for Ped 1-17*

Scan PED, 2-04	Common Scan Quantity	Value
g116313.00800_PED_2-04_4	I_P [MA]	1.4
g116313.00800_PED_2-04_5	B_T [T]	1
	P_{inj} [MW]	8
	dr_{sep} [cm]	-1.5
	Typical Lower Triangularity	0.37

***Table A.13**: Parameters for PED scan 2-04.*

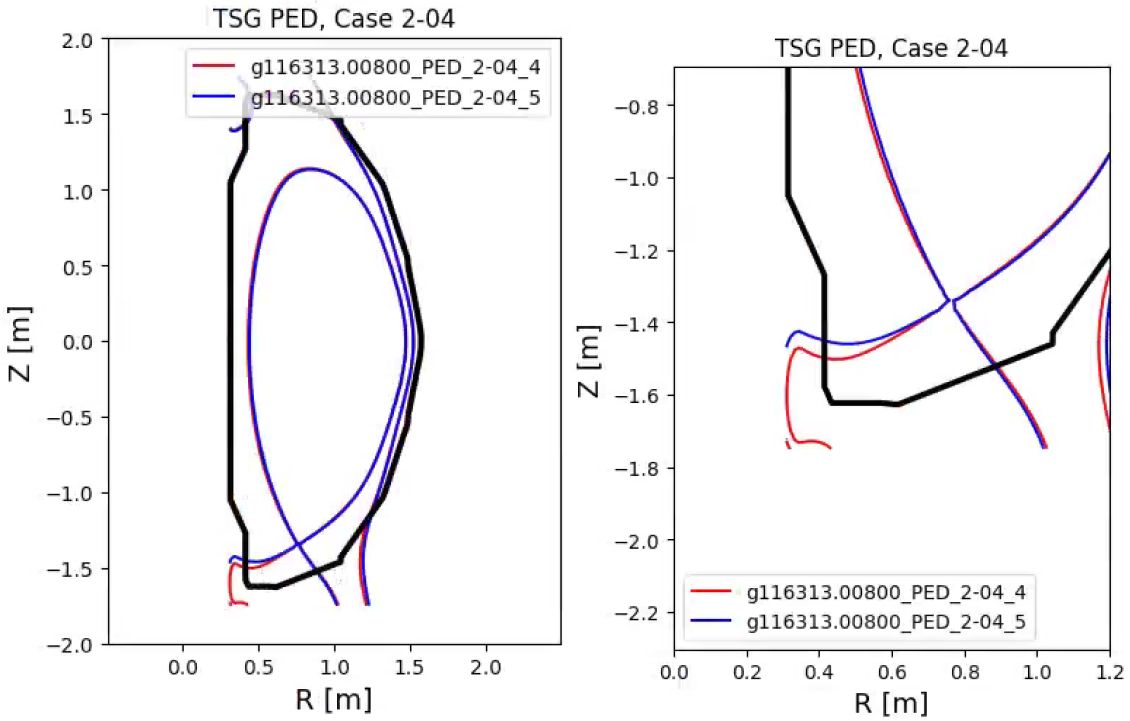

***Fig. A.19**: Equilibria for scan Ped, 2-04.*

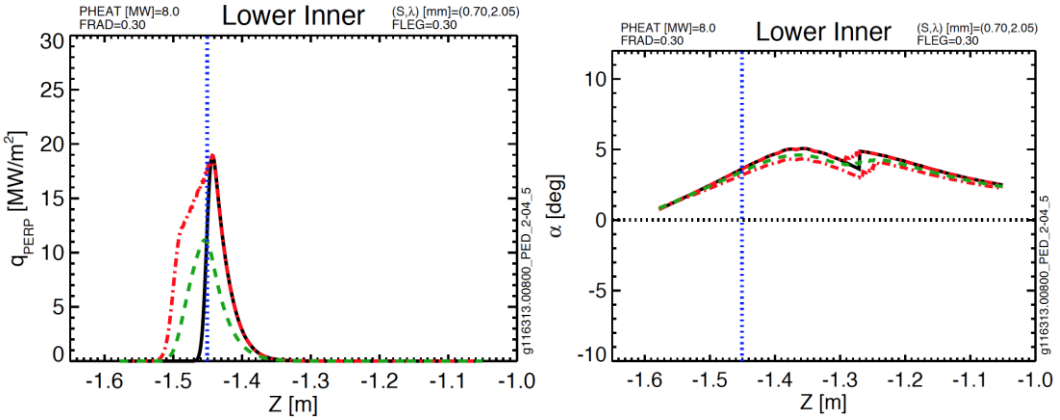

***Fig. A.20**: Lower inner target parameters for Ped 2-04*

Scan PED, 2-05	Common Scan Quantity	Value
g116313.00800_PED_2-05_1	I_P [MA]	1.4
g116313.00800_PED_2-05_2	B_T [T]	1
g116313.00800_PED_2-05_3	P_{inj} [MW]	8
g116313.00800_PED_2-05_4	dr_{sep} [cm]	-1.5
g116313.00800_PED_2-05_5	Typical Lower Triangularity	0.45

Table A.14*:Parameters for PED scan 2-05.*

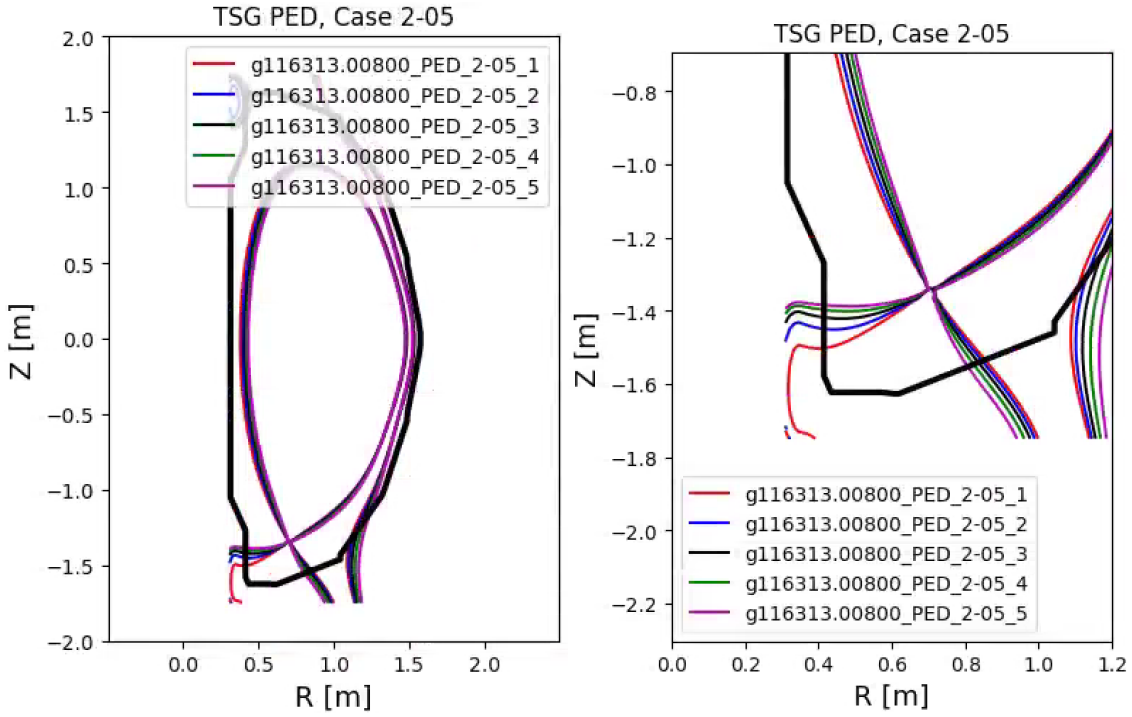

Fig. A.21*: Equilibria for scan Ped, 2-05.*

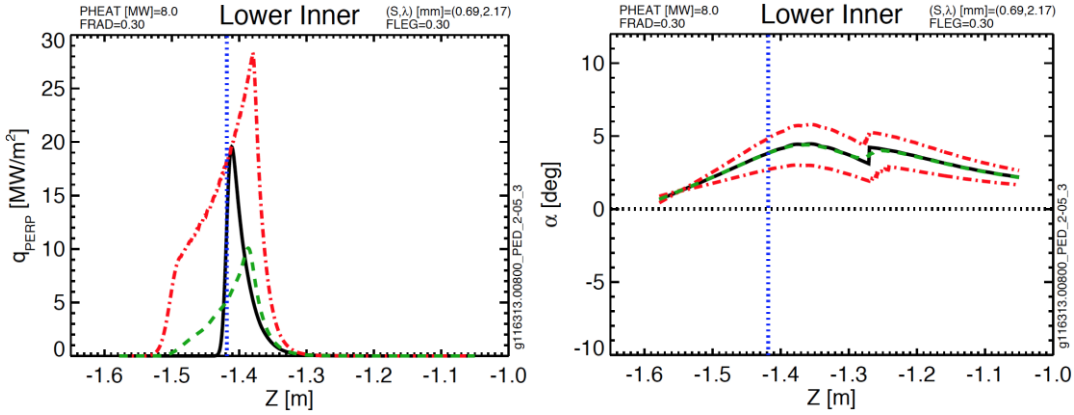

Fig. A.22*: Lower inner target parameters for Ped 2-05*

Scan PED, 2-16	Common Scan Quantity	Value
g116313.00800_PED_2-16_3	I_P [MA]	1.8
g116313.00800_PED_2-16_4	B_T [T]	1
g116313.00800_PED_2-16_5	P_{inj} [MW]	10
	dr_{sep} [cm]	2.36
	Typical Lower Triangularity	0.35

***Table A.15**: Parameters for PED scan 2-16.*

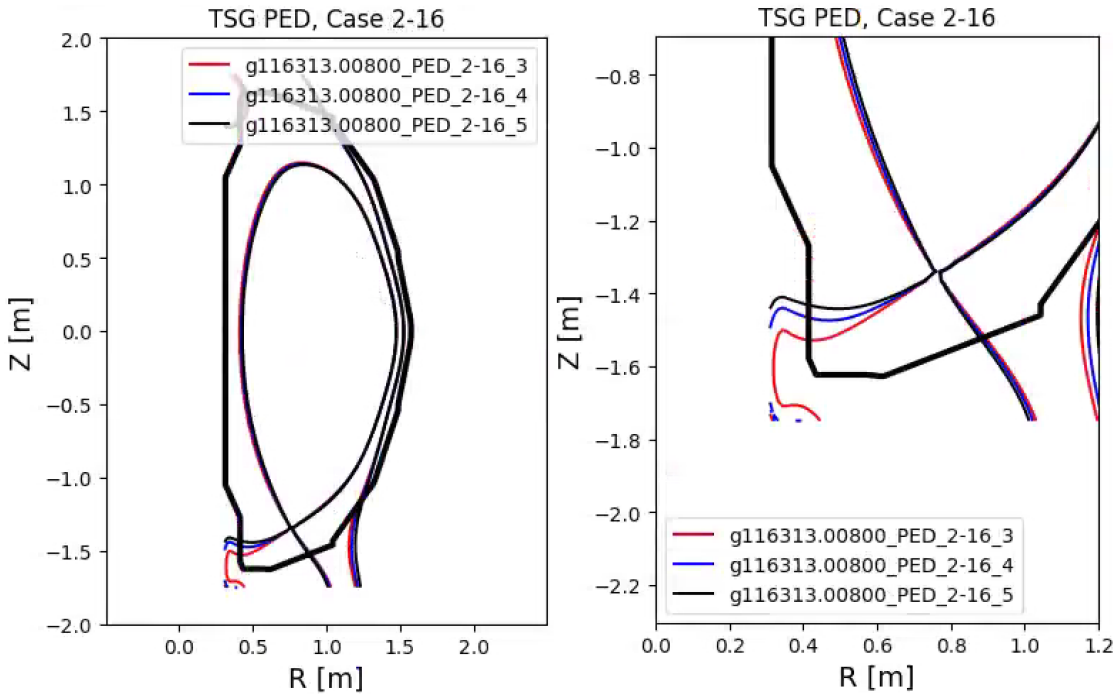

***Fig. A.23**: Equilibria for scan Ped, 2-16.*

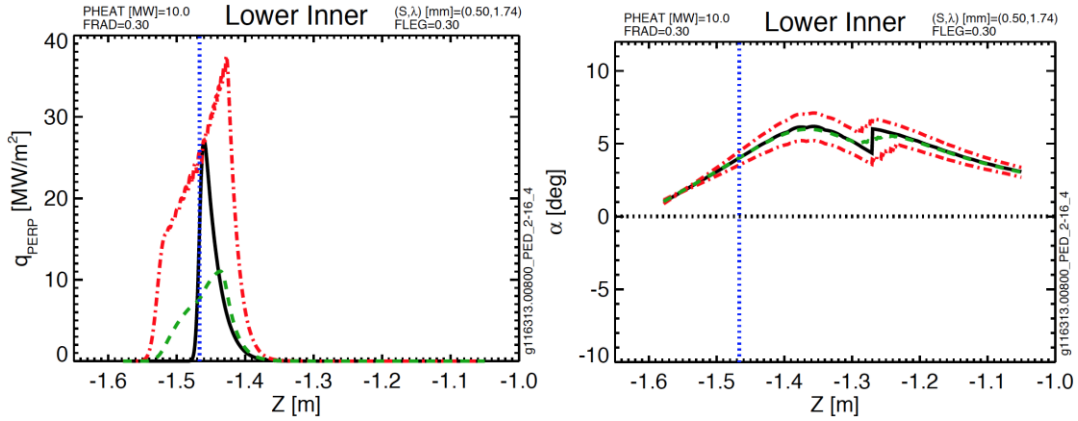

***Fig A.24**: Lower inner target parameters for Ped 2-16*

Scan MPFC, 2-01	Common Scan Quantity	Value
g116313.00800_MPFC_2-01_1	I_P [MA]	1.25
g116313.00800_MPFC_2-01_2	B_T [T]	0.75
g116313.00800_MPFC_2-01_3	P_{inj} [MW]	3
g116313.00800_MPFC_2-01_4	dr_{sep} [cm]	-1.5
g116313.00800_MPFC_2-01_5	Typical Elongation	2.35
	Typical Lower Triangularity	0.5

Table A.16*:Parameters for MPFC scan 2-01.*

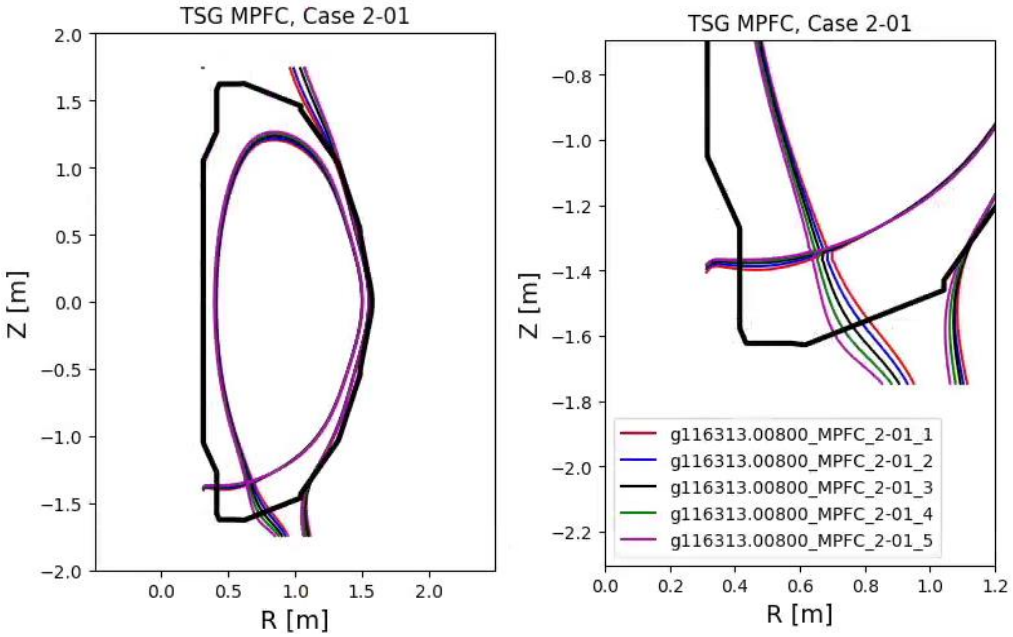

Fig. A.25*: Equilibria for scan MPFC, 2-01*

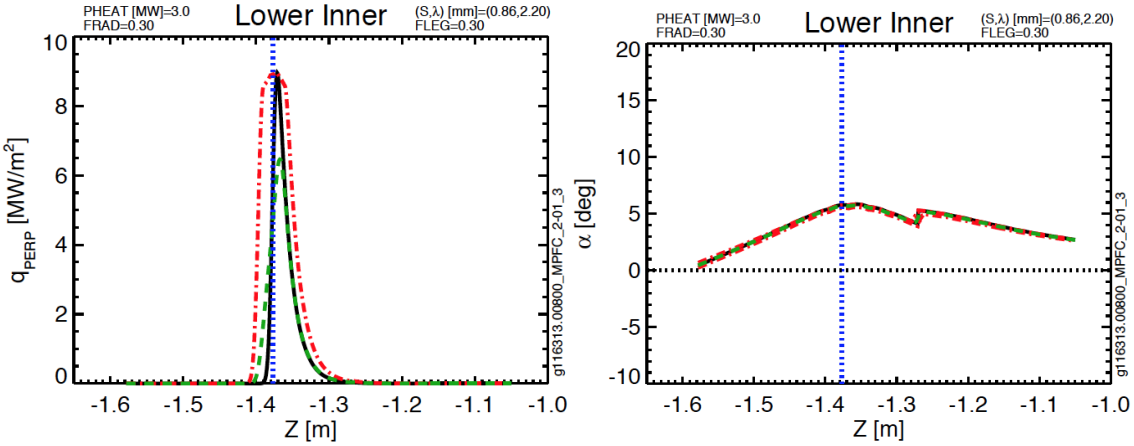

Fig. A.26*: Lower inner target parameters for MPFC, 2-01*

Scan MPFC, 3-02	Common Scan Quantity	Value
g116313.00860_MPFC_3-02_6	I_P [MA]	0.7
g116313.00860_MPFC_3-02_5	B_T [T]	0.75
g116313.00860_MPFC_3-02_1	P_{inj} [MW]	2
g116313.00860_MPFC_3-02_2	dr_{sep} [cm]	-1.5
g116313.00860_MPFC_3-02_3	Typical Elongation	1.9
	Typical Lower Triangularity	0.5

***Table A.17**: Parameters for MPFC scan 3-02.*

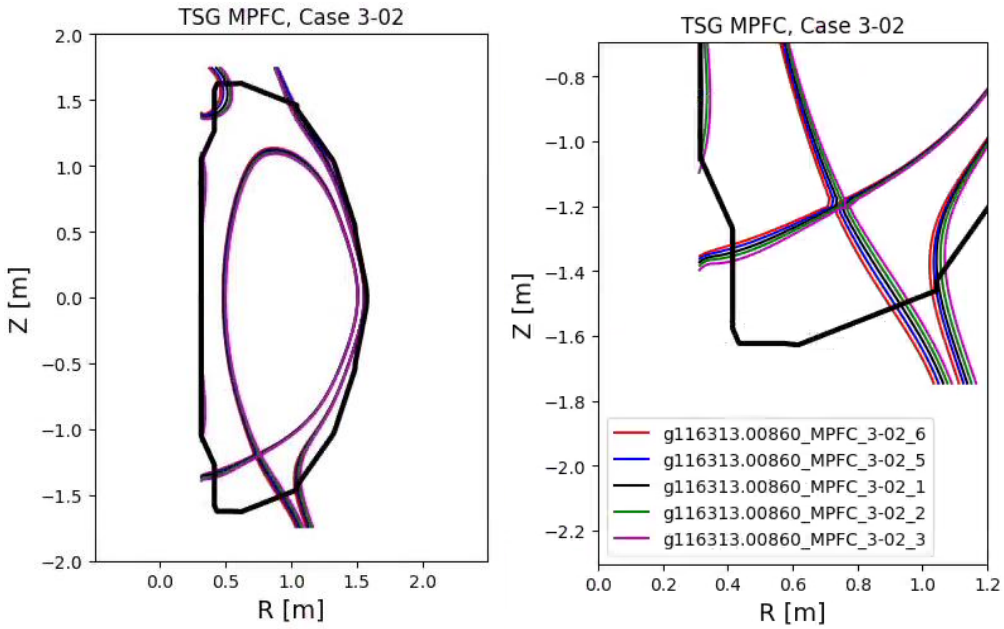

***Fig. A.27**: Equilibria for scan MPFC, 3-02.*

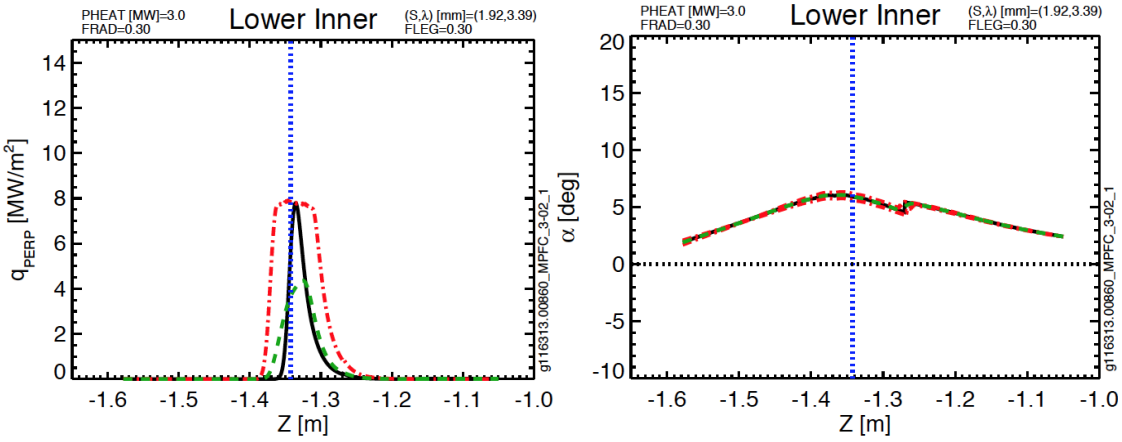

***Fig A.28**: Lower inner target parameters for MPFC. 3-02*

Case 1, Scan 7	Common Scan Quantity	Value
g135111.00500_k2.3_d0.50	I_P [MA]	2
g135111.00500_k2.3_d0.52	B_T [T]	1
g135111.00500_k2.3_d0.54	P_{inj} [MW]	10
g135111.00500_k2.3_d0.56	dr_{sep} [cm]	0
g135111.00500_k2.3_d0.58	Typical Elongation	2.4
g135111.00500_k2.3_d0.60	Typical Lower Triangularity	0.6
g135111.00500_k2.3_d0.62		

Table A.18*: Parameters for Case 1, Scan 7.*

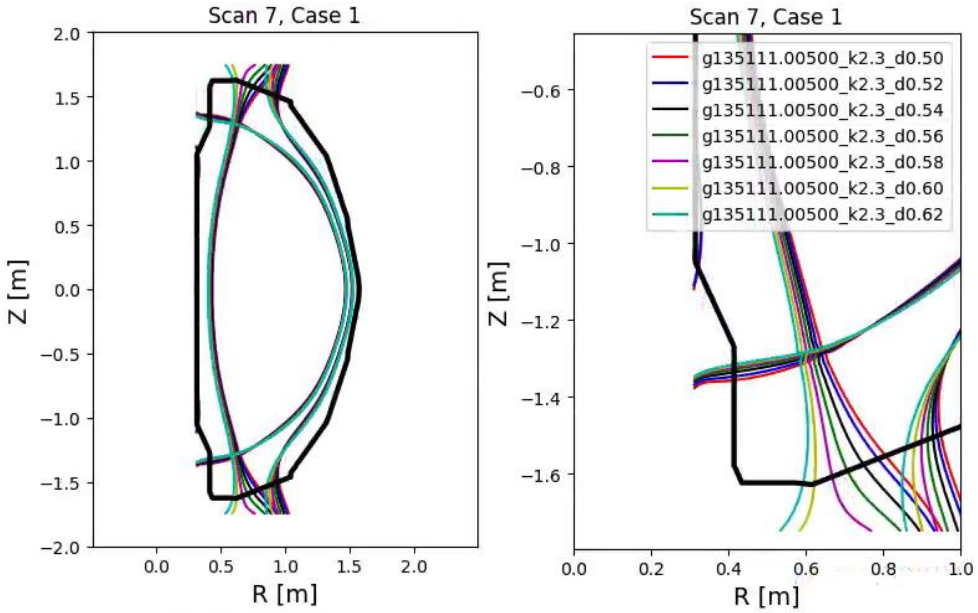

Fig. A.29*: Equilibria for Case 1, Scan 7.*

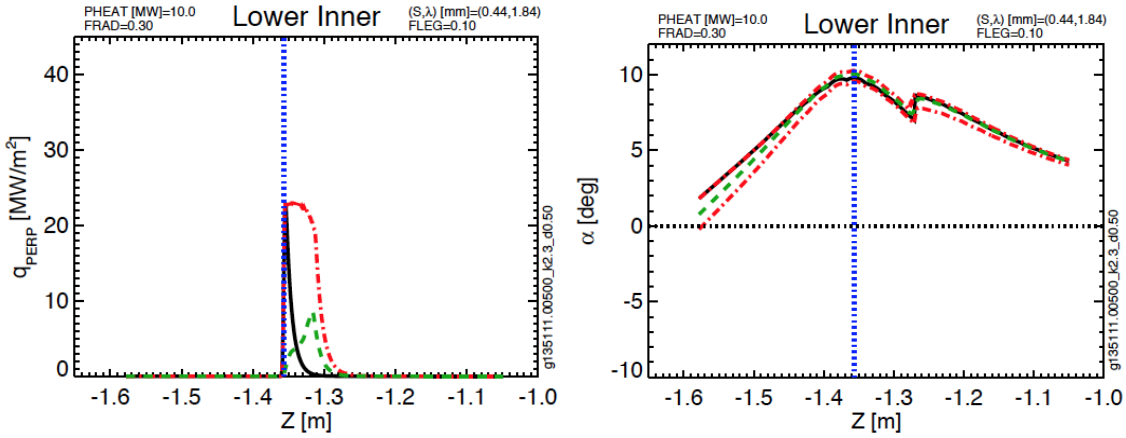

Fig. A.30*: Lower inner target parameters for Case 1, Scan 7*

Case 1, Scan 8	Common Scan Quantity	Value
g135111.00500_k2.4_d0.50	I_P [MA]	2
g135111.00500_k2.4_d0.52	B_T [T]	1
g135111.00500_k2.4_d0.54	P_{inj} [MW]	10
g135111.00500_k2.4_d0.56	dr_{sep} [cm]	0
g135111.00500_k2.4_d0.58	Typical Elongation	2.6
g135111.00500_k2.4_d0.60	Typical Lower Triangularity	0.6
g135111.00500_k2.4_d0.62		

Table A.19*: Parameters for Case 1, Scan 8.*

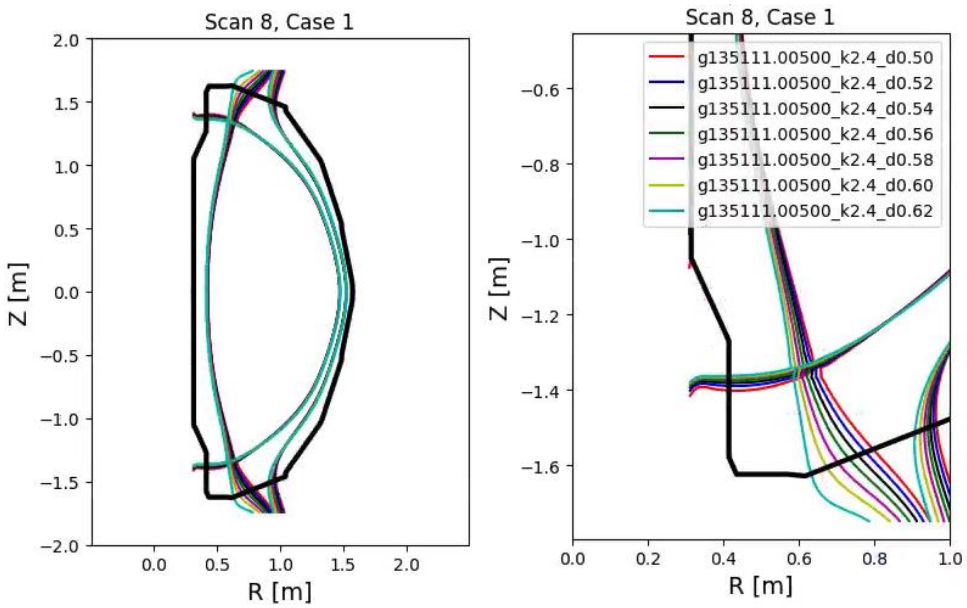

Fig. A.31*: Equilibria for Case 1, Scan 8.*

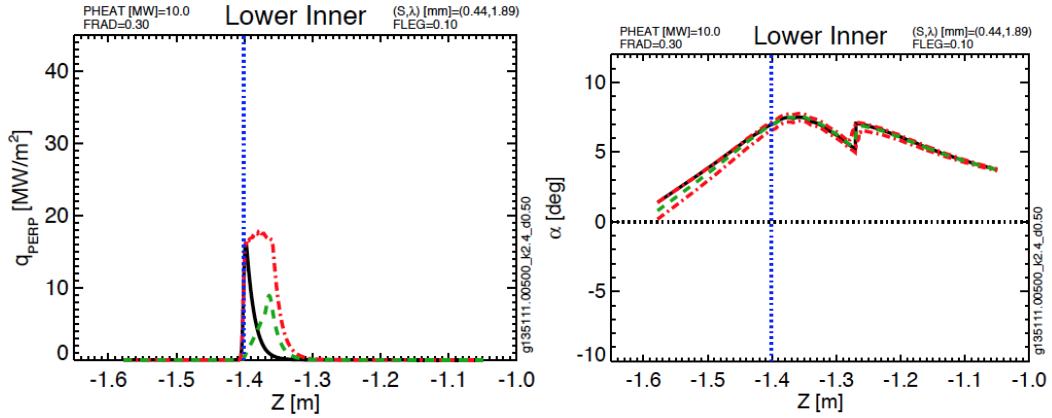

Fig. A.32*: Lower inner target parameters for Case 1, Scan 8*

Case 2, Scan 4	Common Scan Quantity	Value
g135111.00500_k2.55_d0.70_z0.04	I_P [MA]	2
g135111.00500_k2.53_d0.70_z0.08	B_T [T]	1
g135111.00500_k2.51_d0.70_z0.10	P_{inj} [MW]	10
g135111.00500_k2.49_d0.70_z0.11	dr_{sep} [cm]	0
g135111.00500_k2.47_d0.70_z0.20	Typical Elongation	2.5
g135111.00500_k2.45_d0.70_z0.27	Typical Lower Triangularity	0.7

Table A.20*: Parameters for Case 2, Scan 4.*

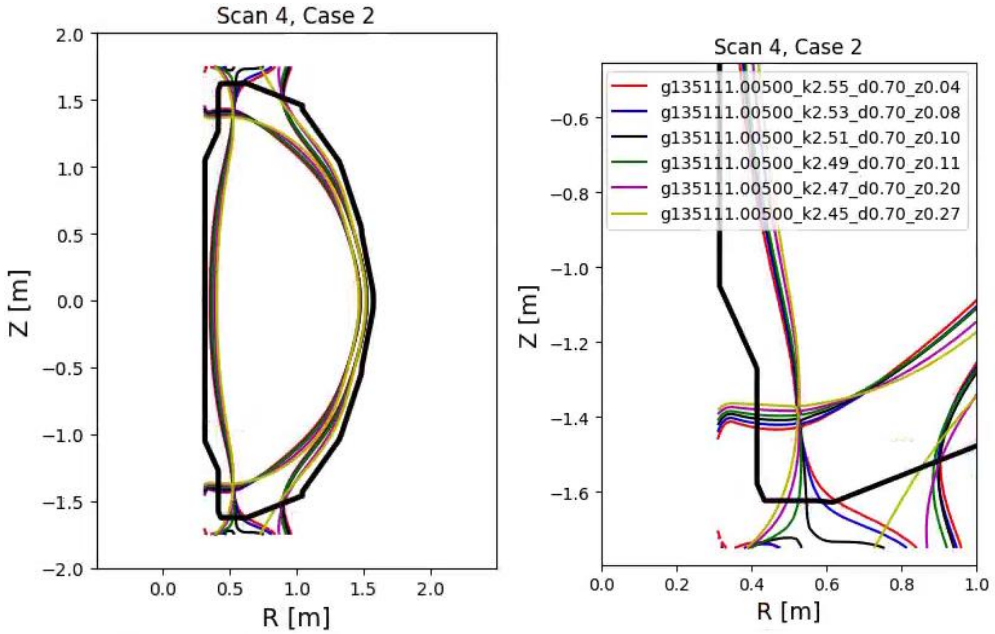

Fig. A.33*: Equilibria for Case 2, Scan 4.*

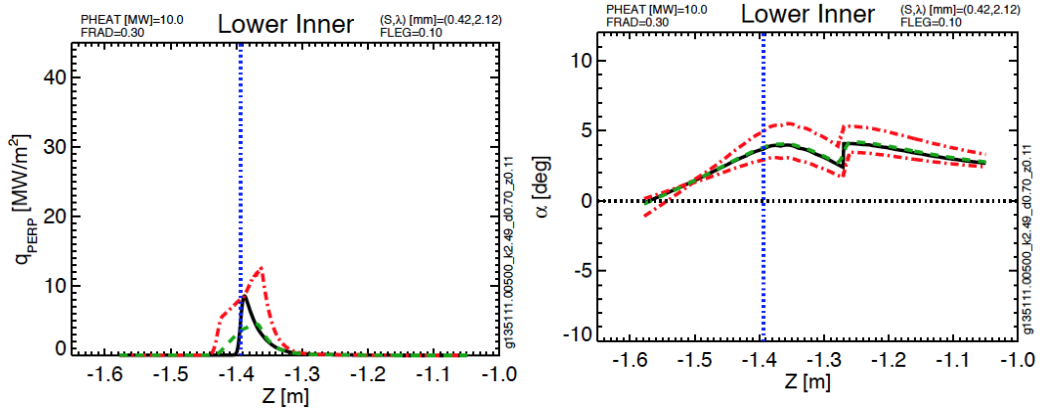

Fig. A.34*: Lower inner target parameters for Case 2, Scan 4*

Case 2, Scan 5	Common Scan Quantity	Value
g135111.00500_k2.63_d0.70_z0.10	I_P [MA]	2
g135111.00500_k2.59_d0.70_z0.12	B_T [T]	1
g135111.00500_k2.55_d0.70_z0.15	P_{inj} [MW]	10
g135111.00500_k2.51_d0.70_z0.25	dr_{sep} [cm]	0
	Typical Elongation	2.6
	Typical Lower Triangularity	0.7

Table A.21*: Parameters for Case 2, Scan 5.*

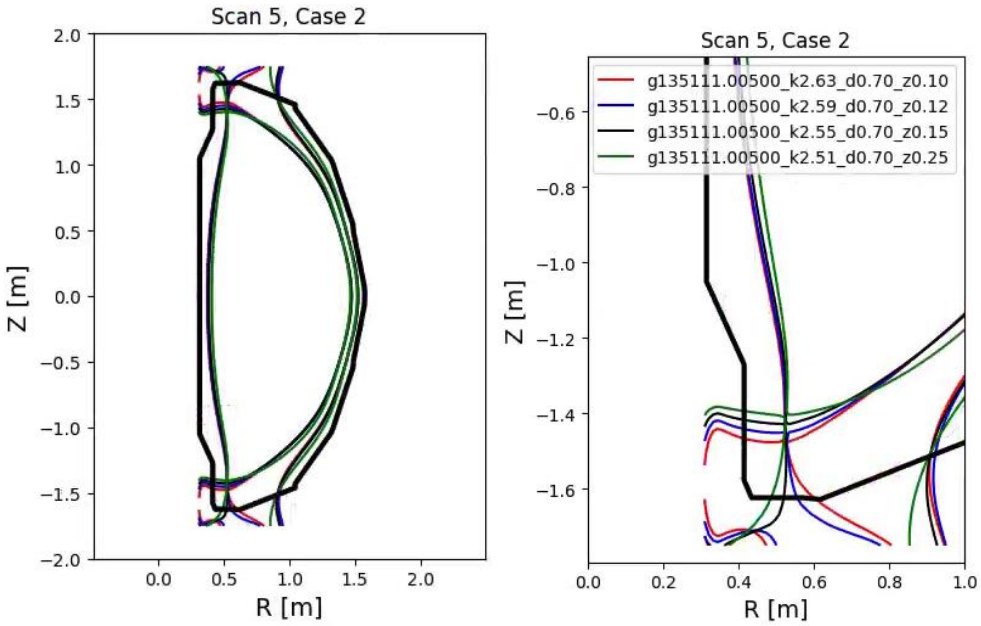

Fig. A.35*: Equilibria for Case 2, Scan 5.*

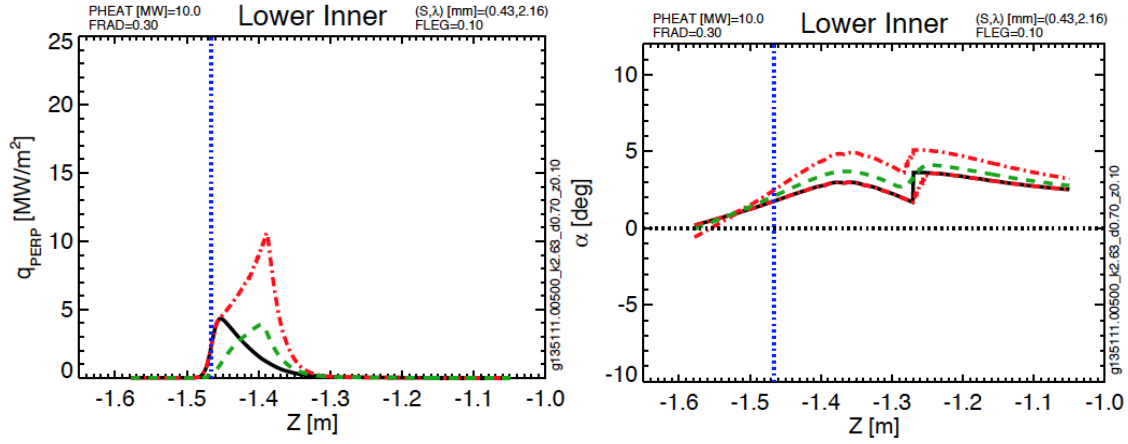

Fig. A.36*: Lower inner target parameters for Case 2, Scan 5*

Case 2, Scan 6	Common Scan Quantity	Value
g135111.00500_k2.67_d0.70_z0.10	I_P [MA]	2
g135111.00500_k2.65_d0.70_z0.13	B_T [T]	1
g135111.00500_k2.63_d0.70_z0.17	P_{inj} [MW]	10
g135111.00500_k2.61_d0.70_z0.20	dr_{sep} [cm]	0
g135111.00500_k2.59_d0.70_z0.25	Typical Elongation	2.7
	Typical Lower Triangularity	0.72

***Table A.22**: Parameters for Case 2, Scan 6.*

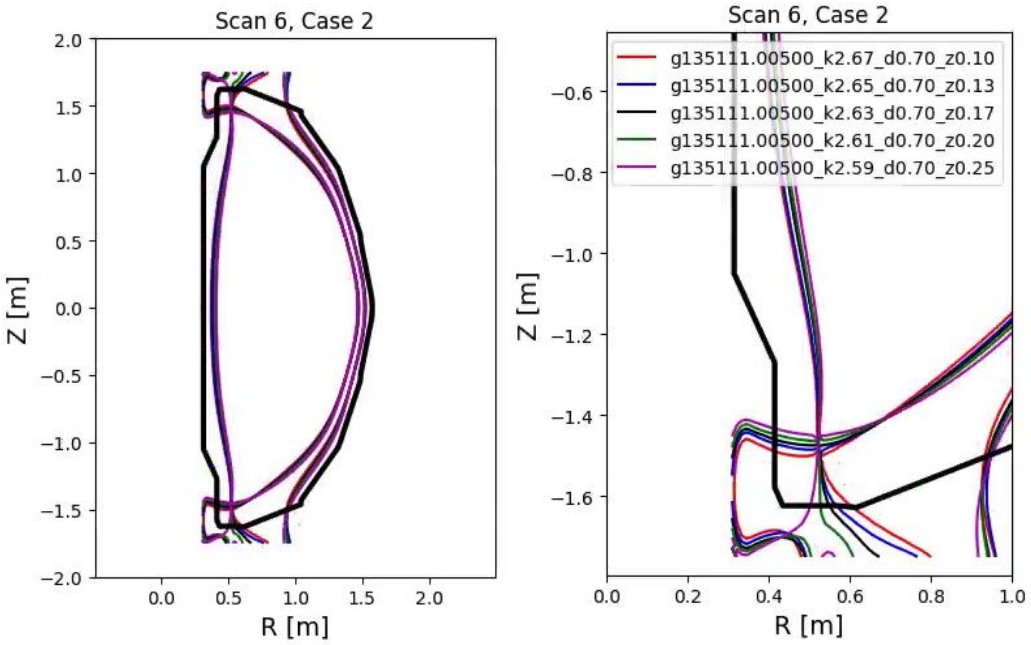

***Fig. A.37**: Equilibria for Case 2, Scan 6.*

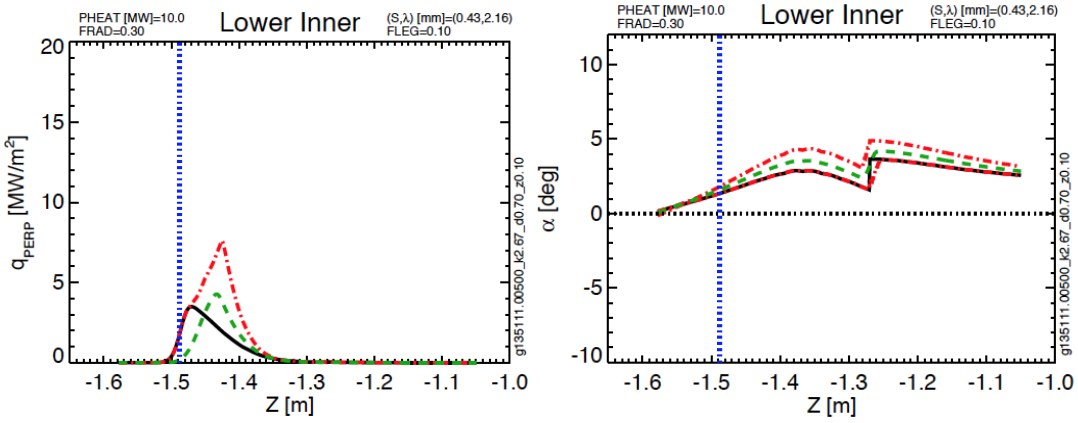

***Fig. A.38**: Lower inner target parameters for Case 2, Scan 6*

Case 3, Scan 1	Common Scan Quantity	Value
g135111.00500_k2.55_d0.70_z0.06	I_P [MA]	2
g135111.00500_k2.53_d0.70_z0.07	B_T [T]	1
g135111.00500_k2.51_d0.70_z0.08	P_{inj} [MW]	10
g135111.00500_k2.49_d0.70_z0.12	dr_{sep} [cm]	0
g135111.00500_k2.47_d0.70_z0.17	Typical Elongation	2.5
g135111.00500_k2.45_d0.70_z0.27	Typical Lower Triangularity	0.7

***Table A.23**: Parameters for Case 3, Scan 1.*

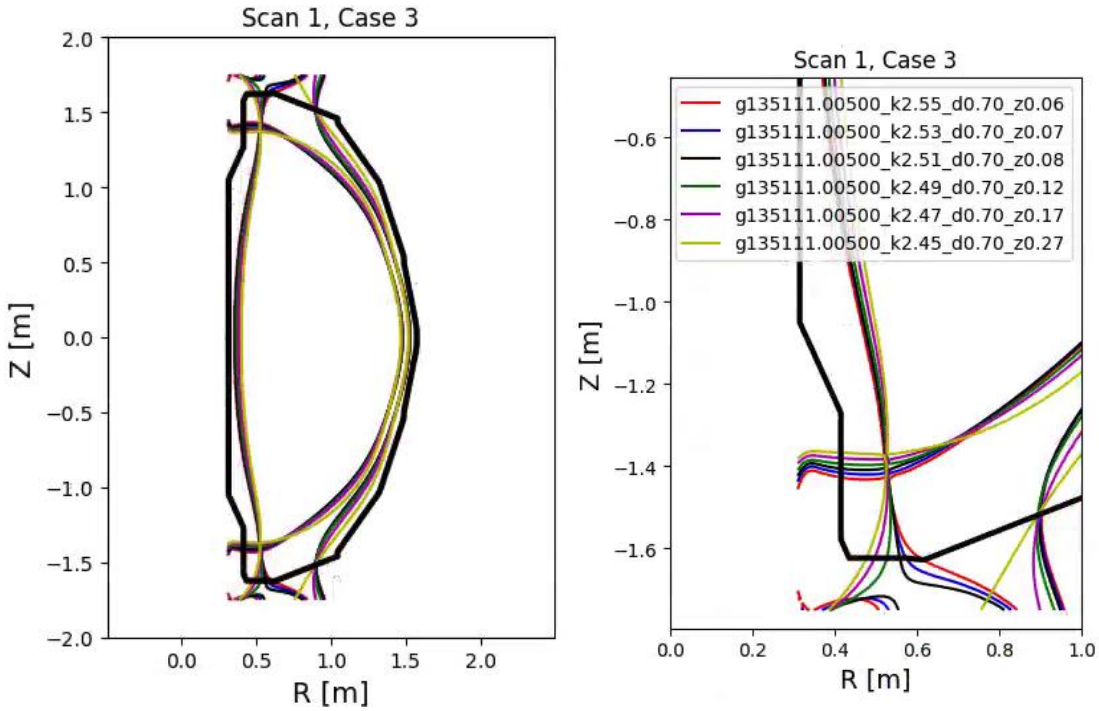

***Fig. A.39**: Equilibria for Case 3, Scan 1.*

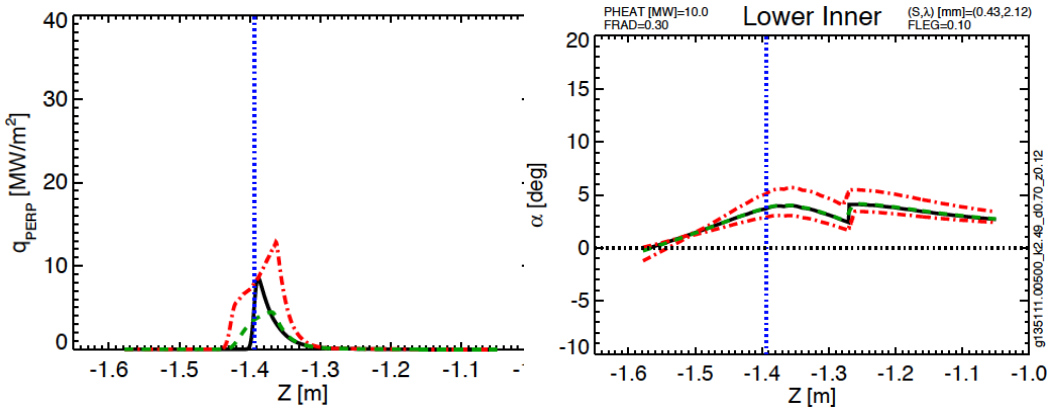

***Fig. A.40**: Lower inner target parameters for Case 3, Scan 1*

Case 3, Scan 2	Common Scan Quantity	Value
g135111.00500_k2.63_d0.70_z0.08	I_P [MA]	2
g135111.00500_k2.59_d0.70_z0.09	B_T [T]	1
g135111.00500_k2.55_d0.70_z0.12	P_{inj} [MW]	10
g135111.00500_k2.51_d0.70_z0.25	dr_{sep} [cm]	0
	Typical Elongation	2.6
	Typical Lower Triangularity	0.7

***Table A.24**: Parameters for Case 3, Scan 2.*

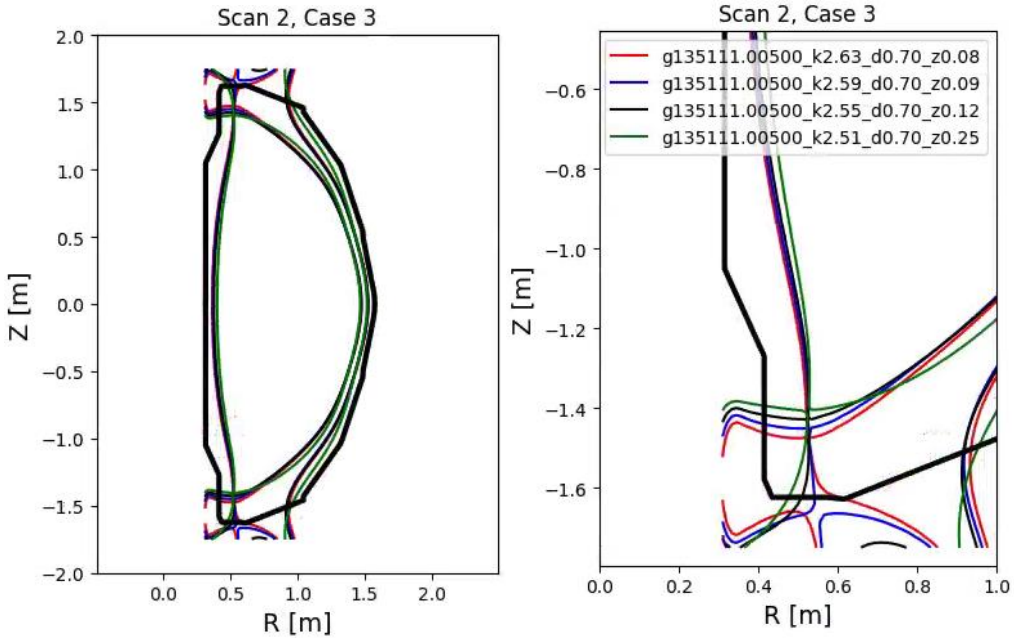

***Fig. A.41**: Equilibria for Case 3, Scan 2.*

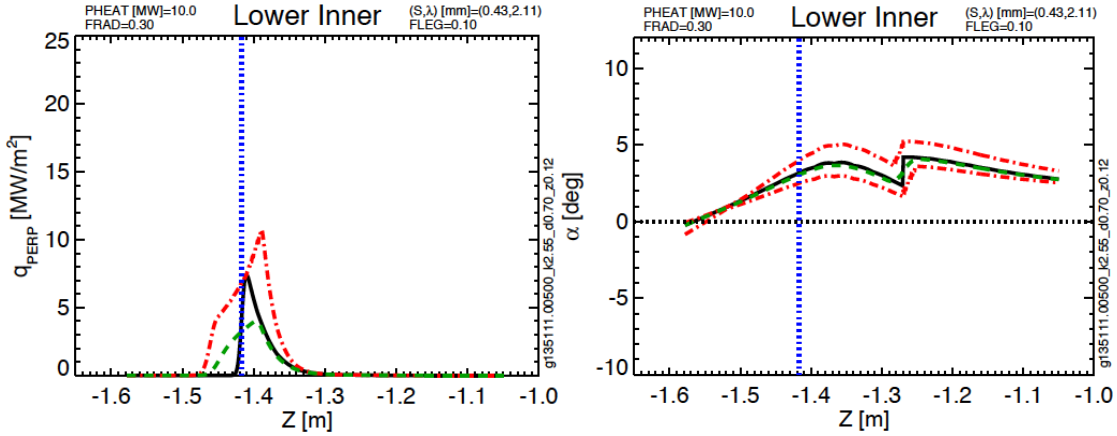

***Fig. A.42**: Lower inner target parameters for Case 3, Scan 2*

Case 4, Scan 1	Common Scan Quantity	Value
g135111.00500_k2.55_d0.70_z0.04	I_P [MA]	2
g135111.00500_k2.53_d0.70_z0.07	B_T [T]	1
g135111.00500_k2.51_d0.70_z0.11	P_{inj} [MW]	10
g135111.00500_k2.49_d0.70_z0.15	dr_{sep} [cm]	0
g135111.00500_k2.47_d0.70_z0.22	Typical Elongation	2.5
g135111.00500_k2.45_d0.70_z0.30	Typical Lower Triangularity	0.7

***Table A.25**: Parameters for Case 4, Scan 1.*

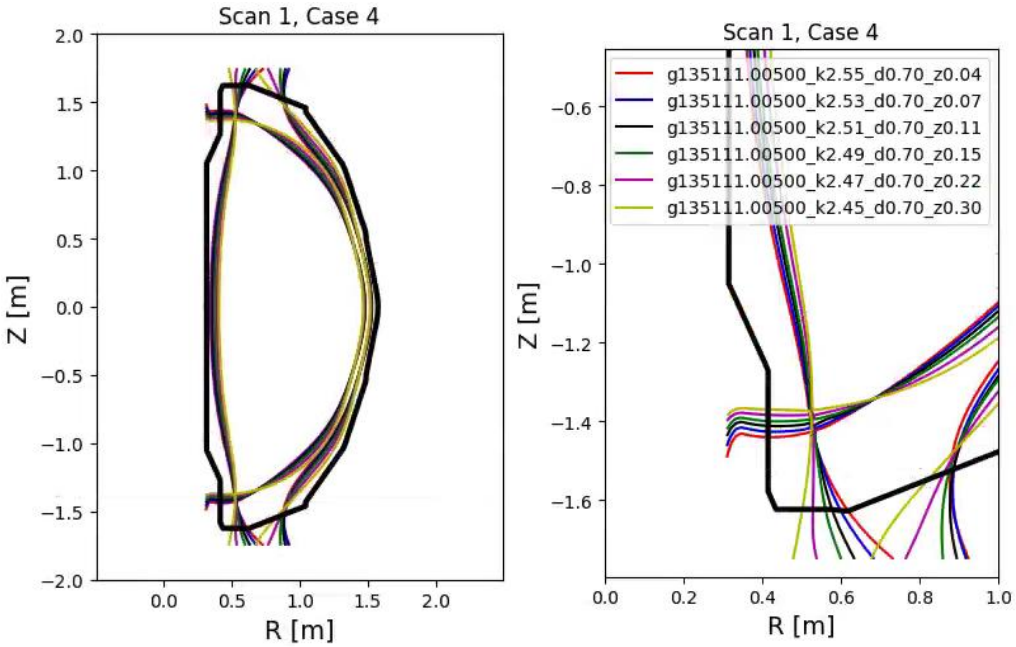

***Fig. A.43**: Equilibria for Case 4, Scan 1.*

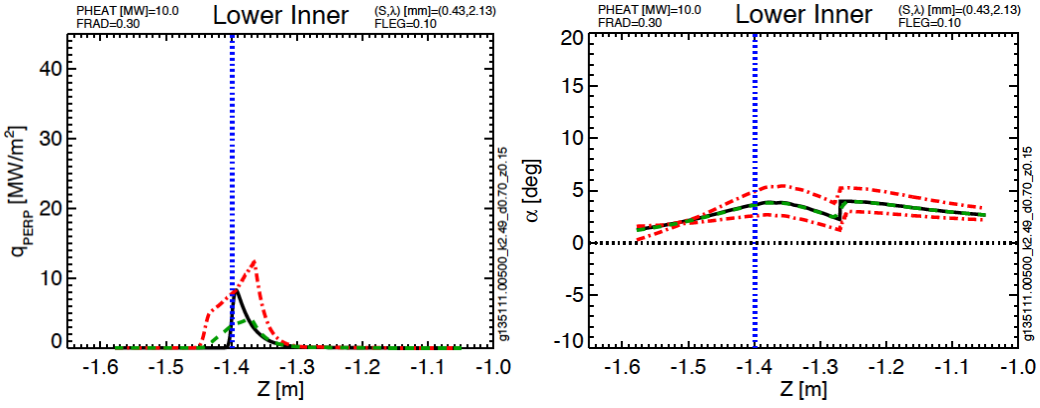

***Fig. A.44**: Lower inner target parameters for Case 4, Scan 1*

Case 4, Scan 2	Common Scan Quantity	Value
g135111.00500_k2.63_d0.70_z0.06	I_P [MA]	2
g135111.00500_k2.59_d0.70_z0.15	B_T [T]	1
g135111.00500_k2.55_d0.70_z0.20	P_{inj} [MW]	10
g135111.00500_k2.61_d0.70_z0.30	dr_{sep} [cm]	0
	Typical Elongation	2.6
	Typical Lower Triangularity	0.7

***Table A.26**: Parameters for Case 4, Scan 2.*

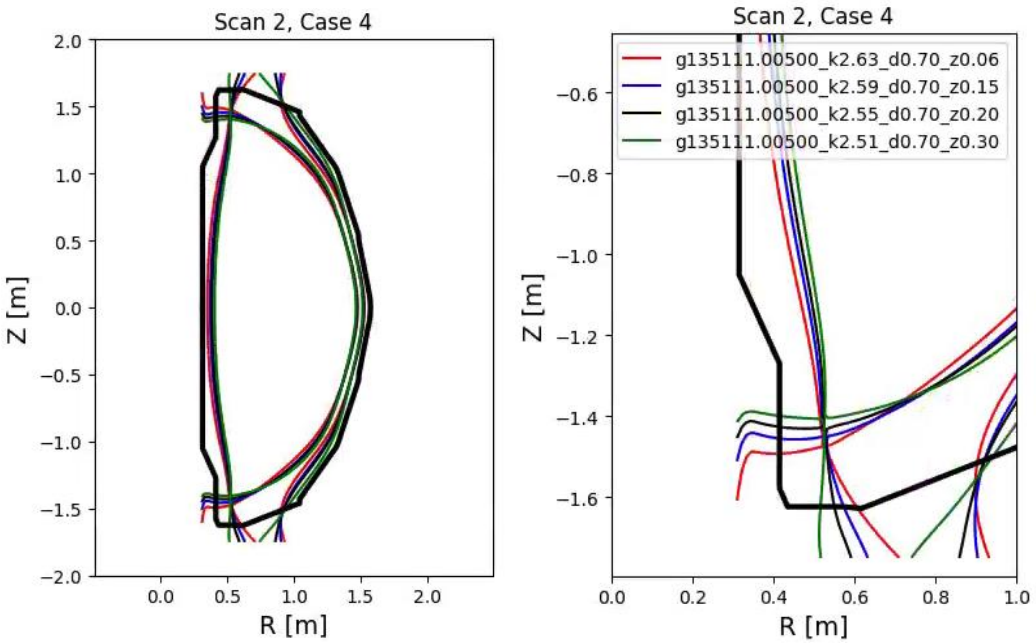

***Fig. A.45**: Equilibria for Case 4, Scan 2.*

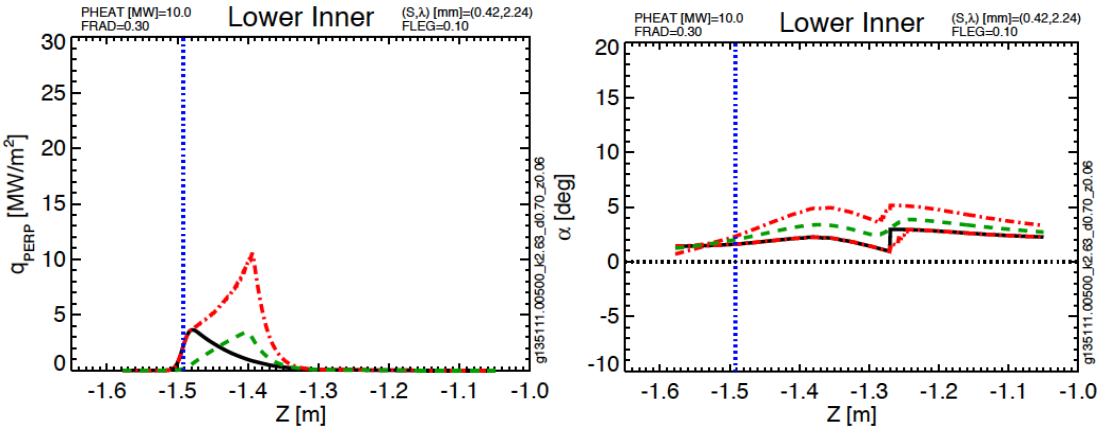

***Fig. A.46**: Lower inner target parameters for Case 4, Scan 2*

Case 4, Scan 3	Common Scan Quantity	Value
g135111.00500_k2.67_d0.70_z0.02	I_P [MA]	2
g135111.00500_k2.65_d0.70_z0.08	B_T [T]	1
g135111.00500_k2.63_d0.70_z0.15	P_{inj} [MW]	10
g135111.00500_k2.61_d0.70_z0.22	dr_{sep} [cm]	0
g135111.00500_k2.59_d0.70_z0.30	Typical Elongation	2.7
	Typical Triangularity	0.72

***Table A.27**: Parameters for Case 4, Scan 3.*

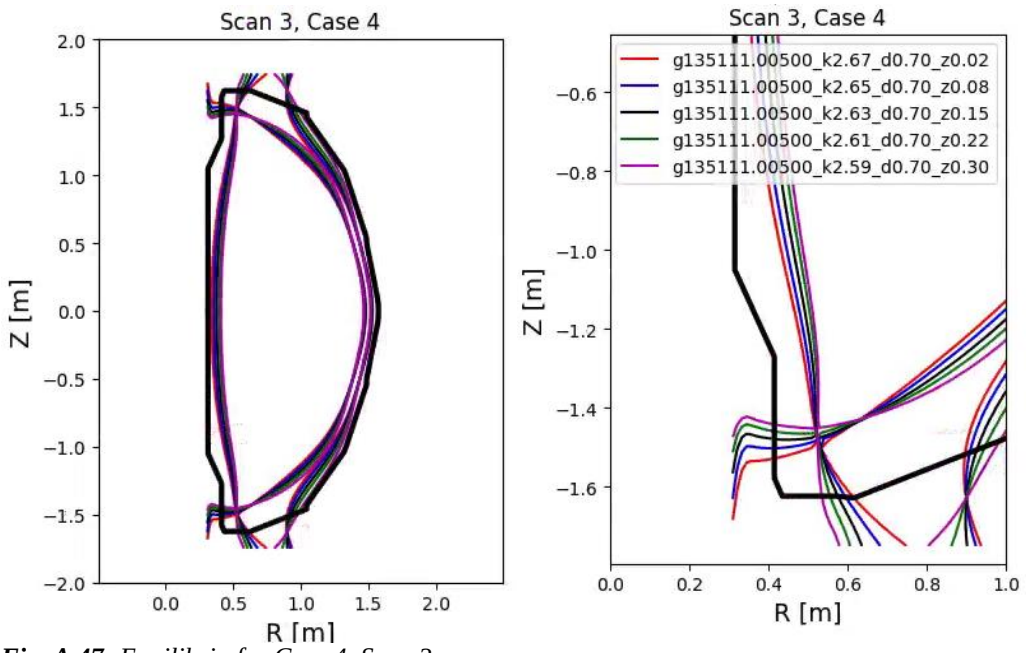

***Fig. A.47**: Equilibria for Case 4, Scan 3.*

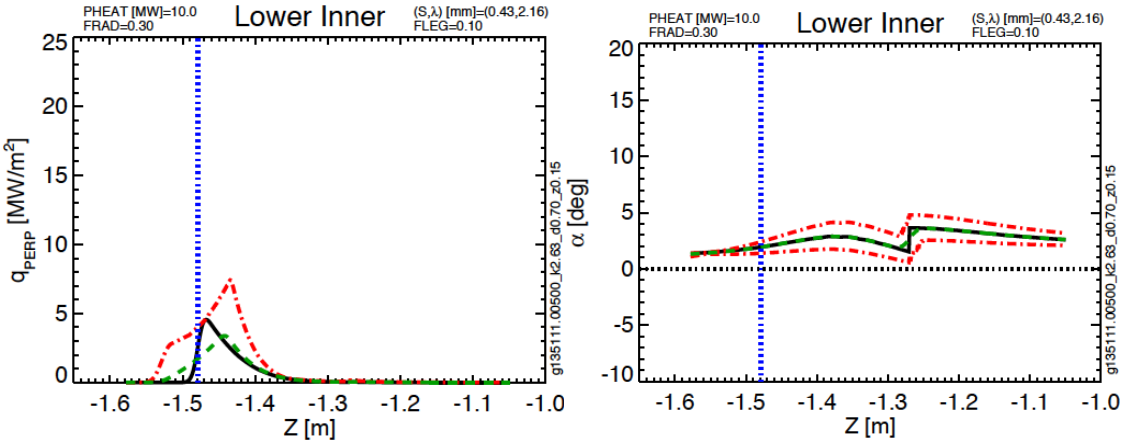

***Fig. A.48**: Lower inner target parameters for Case 4, Scan 3*

Distribution
Jon Menard
Doug Loesser
Mike Mardenfeld
Brian Linn
Ankita Jariwala
Nate Dean
Andre Khodak
Marc Sibilia
Dang Cai
Peter Titus
Art Brooks
Bob Ellis
Filippo Scotti
Vlad Soukhanovskii
Mike Jaworski
Devon Battaglia
Ahmed Diallo
Jack Berkery
Walter Guttenfelder
Stan Kaye
Rajesh Maingi
NSTX-U File